Author's response by Justus G.V. van Ramshorst et al.

13 September 2019

This document contains a point by point reply to review 1 and 2 of the paper by Justus van Ramshorst et al. (DOI: 10.5194/amt-2019-63) and the marked-up manuscript version.

In this document you can find:

REVIEW 1

Review on Manuscript of van Ramshorst et al. 2019 April 20, 2019

Review report: Wind speed measurements using distributed fiber optics: a wind tunnel study

Author of the paper: van Ramshorst et al.
Journal: Atmospheric Measurement Techniques
Manuscript DOI: 10.5194/amt-2019-63

General Comments

The study of van Ramshorst et al. investigated the actively heated fiber-optic (AHFO) technique and estimated its accuracy and precision under controlled airflow conditions by comparing to a three-dimensional ultrasonic anemometer. A very valuable error prediction equation for the wind speed measurements at different heating rates were developed, as the heating rate can be a limiting factor for long cables. This equation is also accounting for averaging over space or time which further increases precision. They conclude that AHFO measurements are reliable in outdoor deployments when correcting the measurements for directional sensitivity with a ultrasonic anemometer, choosing the right heating rate and spatial or temporal averaging. Distributed temperature sensing (DTS) measures temperatures along a fiber-optic cable spatially continuously and can be used in various fields. Especially for atmospheric research this technique offers new insight into the temperature field and thus was implemented in many studies. By using the AHFO technique, wind speed measurements can be added to the system. As the community using the DTS and AHFO technique is growing, the study of van Ramshorst et al. is important for users to be aware of the accuracy, precision and limitation of this technique. Hence, the paper is valuable for our community.

We appreciate your acknowledgment for the importance of our study with AHFO.

The introduction to the determination of wind speed is nicely done, however, I think it can be organized more reader friendly. The overall structure of the paper is logic, but could be reorganized and shortened. In my opinion some figures are redundant. The development of the error prediction equation needs clarification. I could not differentiate results from discussion. Further, I am missing some turbulence statistics of the wind tunnel (friction velocity, velocity aspect ratio, turbulence intensity in different directions to give an estimate how representative the turbulence within the wind tunnel is to outdoor turbulence. I recommend to accept the submitted manuscript after major revisions.

Thanks for your feedback, in the comments below we will reply to each comment.

Title and structure of the paper

Throughout the paper the abbreviation AHFO is used, however the title uses "distributed fiber optics". The title may also incorporate that is not the first paper using the AHFO technique. I propose "Revisiting wind speed measurements using actively heated fiber optics: a wind tunnel study" or similar.

We agree with the suggestion and will revise the title accordingly in the final manuscript

I would propose another order of the sections. After the introduction, I would start with the introduction to the DTS technique and the signal-to-noise ratio (Section 2.4), then introduce the energy balance of the fiber (Section 2.2), then introduce the experimental setup (Section 2.1), because then the reader already know why two fibers are needed, why spatial averaging is potentially important, etc. However, this order is a minor point and could also be chosen differently.

Thank you for the valuable comment, we agree that your suggestion is more logical for the reader and we revise the order into: 2.4, 2.2, 2.1. We would like to add 2.3 (line 1-10) as 2.2.3 were the need for an angle of attack correction is explained. 2.3 (line 11-end) will be added to the results as new proposed angle of attack correction.

Afterwards I would not differentiate between results and discussion. The discussion was insufficient, as I could find no references comparing the work to other studies nor testing or discussing the error prediction equation. I propose to have the following sections instead of Results and Discussion: Directional Sensitivity, Accuracy of AHFO, Precision of AHFO, Error Prediction Equation, Outdoor Deployment of AHFO. Then finally the conclusions.

We agree with the suggestion of reordering the sections and we revise the order into on chapter 3 with the following subsections: 3.1 (2nd part 2.3), 3.2 (old chapter 3), 3.3 (4.1), 3.4 (4.2) and 3.5 (4.3).

I also have specific comments on the following sections:

- Determination of Wind speed (complete Section 2.2):

  The reader is barely able to follow. The equations are introduced in Section 2.2.1, but in the following section the introduced equations are altered or simplified. I suggest to define subsections each concerning one part of the energy balance of the fiber-optic cable, similar to the study of Sayde et al. (2015). Within each subsection all assumptions and simplifications should be noted. This should also shorten Section 2.2.

Considering your comments, we agree that this is a complex section. We did not want to repeat the entire paper of Sayde et al. (2015), however we only summarize its main findings. Nonetheless to guide the reader we propose the combining of 2.2.1. and 2.2.2 into one single section, with the following order and special subsections as follows:

- *Original energy balance by Sayde et al.*
  - *Simplification of the energy balance*
  - *Advective heat transfer coefficient (h) including modifications and assumptions.*
- *Revised simplified determination of wind speed*

We hope this is structure helps to clarify (see revised manuscript)

DTS and Signal-to-Noise ratio analysis (Section 2.4):
I don't see the motivation of this sections besides describing the measurement principle of the DTS technique and sources of noise. Also some sentences are not precise and remain unclear (p.10 l.11, l.17-18, l.20-21) or could be removed (p.10 l.18-19).

We would like to provide the reader some basic information about DTS and more importantly we introduce white noise (temporal and spatial averaging) and the importance of high enough deltaT Furthermore:

- *p.10 1.11: we decided to remove this sentence because it does not add any used information.*
- *17-18: we meant with this sentence that huge temperature differences could create complications related to energy transfer, for example: buoyancy forces become larger. We clarify this.*
- *20-21: we clarified this.*
- *18-19: we changed the sentence*

Using AHFO outdoors (Section 4.3):
The last paragraph belongs into the introduction
We agree and will add it in the introduction after line 5 page 3 (new manuscript).

Questions on deriving the error prediction equation (Sect.4.1&4.2)

The main goal and strength of this paper is the development of the error prediction equation depending on the wind speed, the heating rate and accounting for averaging over space and time. However, in my opinion, the development of this equation have to be presented in a more reader friendly way and the assumptions and the validity of this equation has to be reconsidered. I have some questions concerning the intermediate constants and Eq. 20:

We understand were not clear in our presentation which lead to confusion in this entire section and relates to many of your questions. Therefor we rewrote our results and discussion section (new manuscript). We first explained the revised directional sensitivity equation (3.1). Accuracy and precision are presented in section 3.2. In section 3.3 we normalize the precision results. In 3.4 we present the precision prediction.

The parameter γ is introduced representing σp at 1 s temporal, and 10 measurement spatial, resolution, hence a specific, empirically derived σp.
-> Does this mean that the authors averaged over 10 u_{DTS} measurements spatially? Or did the authors average the temperature differences over 10 spatial measurements? Or did the authors average the temperature of the unheated and heated cable over 10 spatial measurements and from that computed the temperature difference and thus u_{DTS}?

The latter is the case. We averaged 5 heated and 5 non heated temperature measurements and calculated the temperature difference and successively U_DTS from this for every second. We will clarify this in the text. We hope we clarify this with parameters m and k presented in the new manuscript. n_{space} *stands for the amount of spatial measurements, in our case 5. And* n_{time} *stands for the amount of temporal measurements, in our case 1.*

in Eq. 16 γ stands for a specific, empirically derived σp, however, when included in Eq. 20 the same γ is representing σp depending on n, Ps and u_N, which does not seem logical to me. How can the authors defend this?

γ is a function of n_{space}, n_{time}, u and Ps. We removed the use of gamma and introduced equation 15-17 which hopefully clarifies.

$\sqrt{\frac{t_{avg}}{t_{sample}}}$ is $\sqrt{n}$, with n being the number of measurements over which u_{DTS} is averaged over time. This is not mentioned in the text.

This is correct, we explained this in the text by introducing parameter n_{time}.

Following this, Eq. 16 can be rewritten:

$$C_{int} = \gamma \frac{\Delta T}{T_{error}} \sqrt{n} \quad (1)$$

C_{int} is then presented as an intermediate constant, which is also shown in Fig. 9b. However, is C_{int} the mean over all ΔT and attack angles? Fig. 9b shows a spread of C_{int} from 1.3 up to 2.

Yes, this is the mean of all ΔT and attack angles, as we want to present a new constant which can be used as first prediction for all measurements.

Further, did the authors use the constant ΔT or the actually measured ΔT? Please clarify or use different symbols.

We used the measured ΔT. We set the power input such that the measurements had roughly 2, 4 and 6 °C difference.

"By using the shown $\sqrt{\frac{1}{n}}$ dependency, we can easily convert C_{int} into C_{DTS}" (p.15 l.1-2):

- what is C_{DTS} compared to C_{int} or what does it represent?

C_{int} is now defined by equation 18 in the revised manuscript and only considers the temporal averaging. C_{DTS} also considers the spatial averaging, see equation 19.

See section 3.3 in the revised added manuscript

- is n representing the space or time domain in this context?

*For this question we refer to the revised manuscript were we redefined n as n_{space} * n_{time}, which means n is the amount of measurements in time and space.*

C_{DTS} is computed "by multiplying C_{int} by $\sqrt{\frac{10}{1}}$ as n is 10 times less" (p.15 l.2), what is a confusing statement. In my understanding $\sqrt{\frac{10}{1}}$ is $\sqrt{\frac{x_{avg}}{x_{sample}}}$ with x representing the space domain. This is $\sqrt{n_{space}}$ with nspace being the number of measurements over which u_{DTS} is averaged over space. Hence I derive the following equation for C_{DTS}:

$$C_{DTS} = C_{int}\sqrt{n_{space}} = \gamma \frac{\Delta T}{T_{error}} \sqrt{n * n_{space}} \quad (2)$$

We rewrote the calculation of C_{DTS} and introduced the spatial and temporal n_{time} and n_{space}, like you suggested.

in Section 4.2 the goal was to have an estimation for σp. Therefore, Eq. 16 and Eq. 17 are combined, σp is inserted for γ (which is a point of discussion for me as mentioned earlier), solved for ΔT, and inserted in Eq. 19 to derive Eq. 20 when solving for σp.
-> when I did the proposed evolution from Eq. 16 to Eq. 20, I got a factor of $\frac{1}{\sqrt{n}}$, not $\sqrt{\frac{1}{n}}$

Mathematically $\frac{1}{\sqrt{n}}$, and $\sqrt{\frac{1}{n}}$ are the same.
-> in Eq. 20 n "is the number of measurements over which the observed wind speed is averaged, in either space or time domain" (p.15 l.22). However, I interpret this n as n + nspace and not n * nspace (as shown in my Eq. 2). Hence, I think C_{DTS} is computed incorrectly.

*Please consider the revised manuscript, which should clarify that n indeed is n_{space} * n_{time} as in equation 2 of your review.*

-> are the authors proposing that there is also a $\frac{1}{\sqrt{n\_space}}$ dependency for σp? I am missing a figure showing this.

By averaging over space and time the white noise in DTS measurements can be lowered. If the temperature difference and therefor wind speed is (roughly) the same over a spatial distance, averaging over space has the same effect as averaging over time. With averaging over time also uses the assumption that the wind speed stays roughly constant (and in our case the wind speed is constant over time).

-> this changes Fig. 10 completely

As mentioned above, due to our unclearness our equations were misinterpreted and figure 10 does not change completely.

The authors should consider to use different symbols for the time and space domain like n_{time} and n_{space} or similar

We agree and introduced n_{time} and n_{space}, and n as you suggested (see the revised manuscript)

Why did the authors choose γ representing the empirical derived σp when averaging over 10 measurements spatially? As the effect of spatial averaging is also under study in this paper, I would derive σp without spatial averaging, so the lowest possible precision, and then investigate the effects of spatial averaging. Also the derived C_{int} and C_{DTS} seem to be biased by this decision.

We added some explanation to section 2.3 and 3.3 in the revised manuscript where we give an explanation:

Section 2.3: Page 9 line 18 until page 10 line 2.
Section 3.3: Page 4 line 15 until 22

In my understanding C_{DTS} is derived empirically when choosing Ps depending on u_N to have a constant ΔT and C_{DTS} is a mean over all experiments.

This is correct.

This is not considered in Eq. 20 nor further discussed. Is C_{DTS} representing σp for a constant Ps during different wind speeds, even though the experimental design was different and C_{DTS} is a mean over all experiments? Was there an experiment done using a constant Ps verifying the error prediction function?

We did not perform such an experiment. The aim of our study is to determine the heating rate required to have a desired σp for roughly the highest expected wind speed for your application outdoors. For the lower wind speeds the σp will be better, as the temperature difference will be higher and therefor σp.

Do the authors suggest to use a different Ps depending on wind speed? In my opinion it might be not useful in field deployment with quickly varying wind speeds to change the heating rates constantly as the fiber-optic cable needs to reach steady state and there is also a response time between the changed heating rate and DTS measurements. This could potentially lower the precision instead of increasing it.

As mentioned above, the authors suggest to determine one constant heating rate Ps, which is based on the expected highest wind speed and should also be sufficient for the lower wind speeds.

I propose to derive the error prediction function in a more clear way. As shown in Fig. 8 for each ΔT the precision σp is following a $\frac{1}{\sqrt{n}}$-line. Hence, we assume the following dependency:

$$\sigma_p(n) = \frac{\alpha}{\sqrt{n}} \quad (3)$$

with α being a constant different for experiment set up. We found that α depends on ΔT and T_{error}:

$$\alpha = \left(\frac{\Delta T}{T_{error}}\right)^{-1} \quad (4)$$

with T_{error} = 0.25 K being the performance of the DTS dependent constant and ΔT being

the measured temperature difference between the cables. Hence, α is representing the quality factor for the wind speed measurements. The lines derived from α could also be added in Fig. 8. When simplifying Eq. 18 of the submitted manuscript we can assume that ΔT is mainly depending on the following parameter:

$$\Delta T = \frac{AP_s}{Bu_n^m} \quad (5)$$

Combining my Eq. 4 and 5 and inserting that in Eq. 3, I derive the following error prediction equation:

$$\sigma_p(n, u_n, P_s) = \frac{BT_{error}u_n^m}{AP_s}\frac{1}{\sqrt{n}} \quad (6)$$

If I did not miss a point, no empirically derived intermediate constant has to be used for the error prediction equation.

We compared your derived equation with our final equation and concluded that there is a difference, because in our equation there is an additional dependency on the wind speed, because σp on itself is also depended on wind speed (see our equation 14), which not included in your equation 3. With our C_{DTS} we averaged for our wind speed range, which leads to a small difference in estimating the final σp and explains the difference between your eq. 6 and our eq. 22 (revised manuscript)

Terminology

- p.2 l.28-29: "advection of cooler ambient air". I think convective heat loss is the correct phrase here. Please make sure the correct terms are used throughout the manuscript.

We changed this accordingly.

- p.6 l.14: There is a difference between the turbulent Prandtl number and the Prandtl number representing the ratio of momentum diffusivity (kinematic viscosity) and thermal diffusivity. Please clarify.

We meant the latter, see line 20, page 7.

- p.10 l.20:
  "The precision is an indication of the variability of the wind speed (e.g. RMSD),..."
  ! variability of the wind speed can also describe the deviation from the mean wind speed. However, I think in this context the authors refer to the precision of a measurement assuming a constant wind speed.

We agree, we indeed look at the precision of the wind speed measurements and not at the natural wind speed variability. We changed the sentence into:

"The measurement precision is an indication of the variability of wind speed measurements (e.g., RMSD), as opposed to accuracy which describes a systematic measurement error for which van be compensated (in our case expressed by the bias)."

- What is RMSD?

The root mean square deviation, in our case defined in equation 14.

- "... as opposed to accuracy which describes a systematic error that can be removed through calibration (e.g., a bias)."! Accuracy it the combination of trueness (bias) and precision. The accuracy of a measurement can be low due to a poor trueness (high bias) or due to a poor precision. Please adjust throughout the manuscript.

Accuracy can be defined in two ways.

*"**Accuracy** has two definitions:*

1. *More commonly, it is a description of systematic errors, a measure of statistical bias; low accuracy causes a difference between a result and a "true" value. ISO calls this trueness.*
2. *Alternatively, ISO defines accuracy as describing a combination of both types of observational error above (random and systematic), so high accuracy requires both high precision and high trueness." - Wikipedia (https://en.wikipedia.org/wiki/Accuracy_and_precision)*

In our case we use the first definition as can be seen in equation 13

DTS measurements need to be calibrated in post-processing to derive the actual temperatures from the ratio of intensities of Stokes and Anti-Stokes. Hence in this context I would avoid using the word calibration to not confuse the reader.

We change calibration into "for which can be compensated"

p.12 l.13: If RMSD is the root-mean-squares deviation, how was Eq. 15 derived and how does this equation represent the precision? In Eq. 15 the precision of both instruments are combined, even though σp should represent the precision of only the AHFO technique.

The RMSD is derived with the following reasoning:

The measurements of U_{DTS} include the natural and DTS instrument variability
The measurements of U_{sonic} include also the natural variability, and a small (negligible) sonic instrument variability. By subtracting both, the DTS instrument variability is the part which is left.

For clarification we added a line in the revised manuscript

Throughout the manuscript σp is used as a synonym for or parameter representing precision. However, it is counter-intuitive that σp is decreasing for higher precisions.

We understand the point, but mathematically what we do is correct. We will be more careful with the choice of words, by using words like improves or decreases.

Figures

Figure 1: a and b are missing within the figure

Will be changed accordingly.

Figure 2: I would make this figure at least smaller. I don't think this figure is necessary as technical specification of the fiber-optic cable is given in the text.

We think this is useful information for a reader less familiar with DTS. But could be removed on request.

Figure 3: I like this figure very much, however I am missing the connection to Eq. 1. Breaking Eq. 1 into the relevant elements of the energy balance of the fiber and marking those elements with colors or boxes in Fig. 3 makes it even more powerful

We will color the equation in a red and blue part, hence incoming and outgoing energy.

Figure 4: Fig. 4a and Fig. 5a as well as Fig. 4d and 5d are identical. Directional sensitivity is not corrected for an attack angle of 90° angle as this is considered the optimal attack angle, hence showing 4a in this context does not make sense. Why are the symbols different between Fig. 4 and Fig. 5?

We decide to remove figure 4a and only focus on 4b and 4c to visualize the difference in directional sensitivity equation.

For consistency throughout the paper we choose the select one marker per angle.

Figure 5: comparing the subfigures is not easy because they are basically looking the same (also R2 is relatively similar). It is already shown in Fig. 4b and c that the directional sensitivity can be corrected by Eq. 13 and Fig. 5 is not adding new content. I also did not see further description of Fig. 5 nor discussion of it. So I suggest to take this figure out, unless Fig. 5 is described and discussed.

The reason why we would like to add figure 5 is that we would like to show that AHFO works for all angles, without a big reduction of performance as you correctly mention. We added a sentence to the revised manuscript. And we propose to move it to the appendix. (as done in the revised manuscript)

Figure 6: The effects of temporal averaging are shown and discussed in Fig. 8, however this is not done with Fig. 6. Take it out.

We propose figure 6 to the appendix as well. (as done in the revised manuscript)

Figure 7: The symbols are too small to see the filling you are using for different heating rates. Better use opaque colors like in $\Delta T = 2°C$

We will improve the figure.

Figure 8: see comments on Fig. 7

We will improve the figure.

Figure 9: I would rather add $\frac{1}{\sqrt{n}}$ for each heating rate to Fig. 8 than adding Fig. 9a. Each heating rate is following a $\frac{1}{\sqrt{n}}$-decay, so when normalizing by the heating rate the only logical outcome is Fig. 9a. Hence Fig. 9a provides no new content in my opinion. The same appears to me for Fig. 9b.

We think these figures help following the reader in understanding the steps we make to derive C_{INT}.

Figure 10: I would show the same figure, but without spatial averaging. From this paper people should know that the precision can be further increased by averaging spatially or over time.

Since all our figure are based on five sample points, we choose to keep this for consistency.

Specific comments

p.1 l.5 : "operational conditions": I would rather name the conditions: heating rates and attack angles

We add this to the abstract

p.1 l.8-9: Under which conditions? For all conditions?

We added for all conditions

p.1 l.9-12: "We conclude...": no new content. We already know this from Sayde et al. (2015). What is your new contribution?

We change conclude into we confirm. Furthermore, we add one sentence:

"We present a method to guide with AHFO settings in fieldwork preparation, such that data with acceptable precision is acquired."

p.2 l.11: "High-resolution...": add spatially

We changed accordingly

p.2 l.31-35 & p.3 l.1-5: this paragraphs is not well organized

We added a sentence

p.3 l.19-20: "...to create the temperature difference needed to determine wind speed..." a minimum needed ΔT is not determined in this study. I think it is rather: "... to create the wanted temperature difference of at least 2°C..." or similar.

We changed the sentence into:

"An electrical current (I) is passed through the heated cable, to create the temperature difference that is necessary to measure wind speed (ΔT, e.g., 2°C)."

p.3 l.33: "steady state flow" -> maybe add variability of the wind speed from ultrasonic anemometer measurements

Good suggestion, we will add it to the final paper.

p.5 l.5: As you are mentioning the calibration set up here, which calibration set up did you use? single-ended, double-ended or duplexed?

For a single ended setup. We added this to the revised manuscript.

p.5 l.19-20: The captions are identical.

We changed this

p.6 l.11: Why is T_s used for the heated cable while T_f is used for the unheated cable/air temperature? f can be associated with fiber which can cause potential confusion. Maybe use T_a for air temperature and T_f for the temperature of the heated fiber-optic cable.

For consistency we used the notations from Sayde et al. (2015), therefor we would like to keep it like this.

p.8 l.13-15: I do not understand the meaning of this sentence.

This sentence means that the used formula is valid for higher wind speeds.

p.9 l.2-3: "...especially in outside atmospheric experiments." -> I disagree. When using a fiber-harp as a set up like the study of Thomas et al. (2012) to measure wind speeds, attack angles are 90° and no directional sensitivity has to be taken into account.

We do not understand why the setup from Thomas et al. (2012) would completely compensate for the angle of attack. Or do you refer to Zeeman et al. (2015)?

p.10 l.12-15: Why can the measurement error be assumed to be constant in the lab, but not in outdoor deployment? Further, here ΔT is the measurement error of the DTS, while later on p.13 l.13-14 the parameter T_{error} is introduced as the constant concerning the performance of DTS. What is the difference between those two constants?

We agree this was unclear, but $\sigma t = T_{error}$. T_{error} is depending on the DTS machine, and should also be constant outdoors. We remove the second part of the sentence.

p.11 Eq. 14.: what does the overline indicate?

The average over all measurements for one specific wind speed. We clarified this in the new text.

p.12 l.1: what is the "uncalibrated data set"? Uncalibrated DTS measurements? Or were the directional sensitivity of the measurements not corrected?

This is indeed unclear, we meant that the proposed directional sensitivity equation is not yet fully optimized (parameter m_1). To prevent miscommunication, we now leave out uncalibrated.

p.12 l.1-3: why should the energy loss due to free convection be different between different attack angles?

This could be for the same reason that we use a directional sensitivity analysis for calculating the wind speed.

p.12 l.5: even when comparing the other attack angles to the 90°, I can see no clear dependency of the bias. 45° has the smallest bias, while 30° and 15° have more or less the same bias. Hence, I would argue: In hotwire anemometry the bias for small attack angles is high and decreases with increasing attack angle. However, even if this effect is taken into account for AHFO measurements, there seems to be more sources of error causing different behaviour of the bias for different attack angles, but with no clear pattern.

We agree that the bias is not completely solved yet. We point at free convection because all measurements have a positive bias which suggests some energy term is neglected while could not be neglected. Some energy terms might be angle related and some not. Also different temperature differences might influence the amount of energy loss. This requires more detailed investigation in the future, for fully optimizing the method.

p.12 l.8-9: What does "extensive calibration" mean? What else could be done or for what else can AHFO be corrected?

Here is referred to equation 12, but also as mentioned in the comment above further improvement is expected to be possible.

p.13 l.3: "The precision increases to a σp less than 5% by averaging over time" -> where is this shown?

See figure 8

p.15 l.6-7: "However, given the result that the increase in precision behaves independent of ΔT and the averaging time, it is possible to make a prediction for the precision of future work." -> this contradicts Fig. 8 and the derived error prediction equation. The precision only behaves independent of ΔT and the averaging time, when the precision is normalized by both parameter.

What we mean here is that the behavior is the same for ΔT and averaging time, but not necessarily the values. We make use of the behavior to predict the values for other ΔT and averaging times.

p.17 l.2-3: I do not understand the connection of Fig. 10 and the missing factor of free convection in the energy balance of the fiber. Please clarify.

When there is no wind speed at all, the free convection term becomes more dominant compared to the forced convection term.

For clarification we changed to sentence.

p.17 l.9-13: I would add, that either a set up like a fiber-harp has to be used, for which no reference device is needed as the attack angles are 90°, or a reference ultrasonic anemometer or even multiple ultrasonic anemometer have to be used to account for different angles of attack.

If we look at the Zeeman et al. (2015) paper, we understand the fiber harp can compensate for horizontal wind variability (u and v), as we mention in our AHFO outdoors section. However, the vertical wind (w) variability component is not included, which might be important for more complex terrains, like forests.

p.18 l.1-3: Why is complex terrain specifically mentioned, while field experiments with the AHFO technique is valuable in any terrain?

That is true, but what is meant here is that by measuring distributed, more complex flow structures can be captured, compared to with a sonic anemometer, which assumes the point measurement holds for the whole measured area.

Review 2

Interactive comment on "Wind speed measurements using distributed fiber optics: a wind tunnel study" by Justus G. V. van Ramshorst et al.

Received and published: 25 June 2019

General comments

The manuscript describes a controlled laboratory evaluation of a recently introduced technique for wind speed measurements using actively heated fiber-optic cables combined with fiber-optic temperature sensing (AHFO-DTS), similar to hot-wire anemometry. The evaluation considers the wind speed, the angle between the mean flow and the sensing cable and the temperature offset between heated and unheated sections of the sensing cable in the experimental design. The results include a simplified model to help plan the heating requirements for experiments in similar conditions. The study highlights aspects to consider for planning real-world applications of AHFODTS and as a major outcome shows that the potential bias due to sensing cable pitch angle may be low and previously used constants should be reconsidered. However, not all laboratory outcomes can be immediately translated to a real-world field application. The authors added a section to discuss this, but should elaborate on the specific conditions in the wind tunnel (compared to real-world) in more detail, to help the reader. The need to include certain outcomes, particularly time averages of wind speed estimates, is unclear to me. Removing those would improve the focus of the text/figures and reduce redundancy. White noise can be mitigated by spatial/temporal averaging, but the introduction does not clearly mention the relevance for this study; I think that the outcomes for high-end resolutions of AHFO-DTS (currently 1Hz, 0.3m) are conclusive enough without it. After major revisions the manuscript should be considered for publication, and I expect it to be a very helpful contribution for those interested in spatial wind speed measurements using this novel technique.

Thank you for your kind words and constructive comments.

Thanks you for your suggestion to elaborate on the specific conditions in the wind tunnel. We will add turbulence statistics of the wind tunnel in the new paper, as also suggested be reviewer 1.

We agree averaging over time and space was unclear, but in the revised paper we tried to solve this. By explaining the need to C_{DTS} we need to average over time and space. Finally, with these results we present a method for estimating the precision of future experiments. We now emphasize this more throughout the manuscript.

Specific comments

In their current form, Fig 4, 5 and 6 do not adequately highlight the differences between the applied corrections or experimental settings. Actually, the uncorrected regression (Fig. 4a) fits the range of observations in the center, making it look like a better fit. Please improve the figures.

We agree and would like to point at the proposed changes to remove figure 4a and figure 5 and 6 to the appendix. See also see comments review 1.

The reason to present results for different averaging periods was not clearly introduced. I suspect those averaging details can be left out and this would help focus the result/ discussion section (remove Fig 6 through 9). The precision and accuracy are most meaningful at the highest resolution, for combinations of different angle, wind speed and temperature offset (and heating rate) settings, and could perhaps be summarized in a single figure or table.

Please consider the answer above why we average over time and space.

A fixed temperature difference between the reference and heated probe would require a feedback system that adjusts the heating rate according to previous or expected wind conditions.
1.In the laboratory setup, was this adjustment in heating rate made manually or automatically How accurate could this be set and were heating rate readjustments made during the 10-min steady periods? The text suggests that under low angles of attack, the heat exchange is less efficient and, consequently, a lower heating rate can be applied to achieve a 2/4/6 K differences compared to the reference. Please discuss the impact of such variable heating rates on the results.

For each wind speed setting we manually choose a heating rate which roughly gave a 2,4 or 6 °C difference. During this experiment the heating rate was not adjusted.

It is indeed correct that the heat exchange is less efficient with small angles. We compensate for this directional sensitivity with our directional sensitivity equation 12. Also C_{DTS} for our final equation includes this.

2. In real-world applications, with more variable wind and radiation conditions, such a feedback system may become challenging. A constant heating rate (variable temperature difference) is perhaps more practical. Therefore, could you also present your results expressed as a function of heating rate, instead of fixed temperature offset?

In our experiments we already work with a fixed heating rate to create the temperature difference. As we discuss AFHO outdoor section we propose that for outdoor applications you estimate the maximum expected wind speed and based on this choose one desired precision, which results in one heating rate which should be sufficient.

In the end equation 22 (revised manuscript) contains the heating rate.

Section 2.2.2 includes both a modification - a different set of constants - and a simplification of the set of equations from Sayde et al (2015) for applications in a wind tunnel. This is not reflected by the section title. Perhaps move the proposed modification (with figure) to the results section or rephrase the section title.

Thanks you for this suggestion, this is changed in the revised manuscript

Why were there no (additional) reference measurement made downwind of the heated cable? In a controlled environment, this could help identify feedback between ref and heated cables in relation to separation distance. In a real-world application, would this make a setup less sensitive to wind direction shifts, or is the relative position of both sections irrelevant? Given the long-standing expertise among the authors, could further recommendations be made for follow-up evaluations of AHFO-DTS inside or outside the wind tunnel?

In this study was focused on a one-dimensional case to study in detail the precision of the method. In the AHFO outdoor section we already make some suggestion to use 3D AHFO set ups to make the method less sensible to non-perpendicular wind directions.

Technical corrections

p1l1/p1l15: Either Active or Actively, choose one for the AHFO definition.

We will use Actively.

p2l21: remove the comma after '(2015)'

Removed

p3l16: 'cable (which encloses the FOs)': suggestion 'FO cable'

We changed this into fiber optics

p3l27: 'angles of attach': suggestion 'angles of attack with the mean flow'

Good suggestion, we add angles of attack with the mean flow direction.

p3l27: Were the ref and heated cable also 8 cm apart in mean wind direction under these slanted angles? From the following sentences this is not immediately clear. If not, would it matter if they would come closer together? Please explain.

Yes, the separation distance was always 8cm. We will add a top view picture in figure 1.

p3l33-p4l1: 'The wind speed in the wind tunnel was fixed at a constant value to create a steady state flow.': perhaps remove, or rephrase to be more specific. Do you mean: The engines in the wind tunnel were set to a constant rate, generating a steady (often laminar) flow after some time and, as a result, a dynamic steady state heat exchange of the FO cables with the moving air.

We mean that the wind speed in the wind tunnel is at a fixed wind speed. In the final paper we will add some turbulence statistics.

p4l2: This paragraph contains a listing of three different experimental settings. Please help the reader by presenting them as such. 'First,... Second,. . .' or other rephrasing.
p4l2: 'Furthermore, for all wind speeds and angles the temperature difference between the reference and heated section, delta T, wat set at 2, 4 and 6 K in order to evaluate the importance of hotwire signal magnitude.'

We changed this sentence

p4l8: 'machine': maybe 'instrument'?

We prefer machine for consistency.

p4l9: 'One cable segment was heated.', suggestion: remove this first sentence and rephrase the second sentence 'The stainless-steel casing of the heated section was ...'

We rephrased the sentence

p4l10: Steel or other wire material?

The AWG cables are from copper, we added this.

p4l11: a temperature difference should be reported in K (Kelvin). Also, those values were already mentioned. suggestion: change ' to a fixed level, either 2, 4 and 6 °C, depending on the setup' to 'at fixed levels'.

We will change degree C to K in the final manuscript. Also we changed the sentence.

p5l4: what is an 'ambient bath'?

A bath which is at room/air temperature, which is needed for internal DTS calibration.

p4l7/p5l8: double ended DTS measurement was applied (p4) but not used (p5). Please put these details together in a single paragraph. Are there quantitative criteria to reject the double ended method using the arguments here, perhaps described in literature (citation)?

During analysis at was found that the signal loss at the splice was not symmetric/clean. Therefor based on expert judgement we decided it was safer to not use this data.

p5l21-p5l22: Somewhat vague. 'An energy balance ... advective energy transport from the heated cable, ...'. suggestion: 'An energy balance method ... heat dissipation from the heated section, ...'. The heat dissipation may not be a fully advective process.

We rephrased the sentence.

p6l14: please rephrase, introduce the abbreviation last, suggestion: 'The Nusselt number, Nu, is the ...'

We rephrased it.

Match the citation style according to journal guidelines, throughout the text. Particularly the year notation with nested parenthesis seems odd, p2l3 should be "... (e.g., Goodberlet et al., 1989)".

We will check this and change if necessary

- Fig. 4, Fig. 5, Fig. 6: Add a meaningful indication of the statistics of these point clouds - add means, or convert the presentation to boxplots - or remove the figures.

We decided to remove and replace the figures to the appendix as mentioned.

- p10l1-p10l21: contains details already mentioned before and details that should better be placed in an introduction.

We restructured the whole method section in the revised paper.

- Eq 12 and 13: where is u_N defined?

See equation 10 in the revised manuscript, we changed the description of this equation.

- p10l26: Is the center of the wind tunnel cross section also the center of the ref/heated FO cable sections?
Why use a section of 0.9 m and not 0.3 m, the advertised resolution of the system, nearest to the location of the sonic anemometer sensor path?

Please show that the extended spatial range did not have an impact on the outcomes. Also, by taking a fixed length of FO, the observed positions in the cross section of the tunnel changed with angle; the 15 degrees angle of attack setting would only integrate approximately 0.2 m vertically.

Since the bottom of the fiber was attached to the tunnel (p3l26-30), were the positions of the center of the ref/heated sections determined at different positions along the optical-fiber length for each angle?

Yes, this is always in the center.

Please consider the changes in the revised manuscript as mentioned in review 1.

We will add a table to the new manuscript which shows that this extended spatial range is justified.

We always used the 5 measurements close to the sonic and in the middle of the wind tunnel. So this changes for every angle.

p10l26: 'Only the temperatures from the middle of the wind tunnel are used, to prevent using data with side/boundary effects.' If the center of the observed sections, independent of the angle of the cable, were centered at the same position in a cross-section of the tunnel as the sonic anemometer, please state this explicitly in the method section.

We added a sentence stating this: We always used the 5 measurements closed to the sonic and in the middle of the wind tunnel.

p10l27: Referring to 'data' here is not very specific, please rephrase. suggestion: 'AHFO-DTS derived wind speed estimates'.

We changed this accordingly.

p10l28: Averaging to 30 sec, including Fig. 6+7, shows no new information: better to leave it out?

As mentioned Figure 6 will be moved to the appendix. Figure 7 is important because it shows the bias difference between different angles.

Fig. 5c: In the review copy, it seems like the 16 m/s data included values that had not reached steady state yet (variability in Usonic, < 16 m/s). Could you please verify?

We will check this for the final paper.

p12l11: 'The precision is calculated for all 120 à T , angle and wind speed combination, using Eq. 15.' Please refer to the equation after it has been defined.

We will move this equation.

- p13;14: Are these numbers for Terror computed, based on the calibration bath sections? Or a specification of the instrument?

These are given by the instrument specifications.

Marked-up manuscript version

The marked-up manuscript version of van Ramshorst et al. (2019)

~~Wind~~ Revisiting wind speed measurements using ~~distributed~~ actively heated fiber optics: a wind tunnel study

Justus G.V. van Ramshorst[1,4], Miriam Coenders-Gerrits[1], Bart Schilperoort[1], Bas J.H. van de Wiel[2], Jonathan G. Izett[2], John S. Selker[3], Chad W. Higgins[3], Hubert H.G. Savenije[1], and Nick C. van de Giesen[1]

[1]Delft University of Technology, Water Resources Section, Stevinweg 1, 2628 CN Delft, The Netherlands
[2]Delft University of Technology, Geoscience and Remote Sensing, Stevinweg 1, 2628 CN Delft, The Netherlands
[3]Oregon State University, Biological and Ecological Engineering, 116 Gilmore Hall, Corvallis, Oregon 97331, USA
[4]University of Göttingen, Bioclimatology, Büsgenweg 2, 37077 Göttingen, Germany

Correspondence: Justus van Ramshorst (justus.vanramshorst@uni-goettingen.de)

Abstract. Near-surface wind speed is typically only measured by point observations. The Actively Heated Fiber-Optic (AHFO) technique, however, has the potential to provide high-resolution distributed observations of wind speeds, allowing for better characterization of fine-scale processes. Before AHFO can be widely used, its performance needs to be tested in a range of settings. In this work, experimental results on this novel observational wind-probing technique are presented. We utilized a controlled wind-tunnel setup to assess both the accuracy and the precision of AHFO under a range of operational conditions (wind speed, angles of attack and temperature difference). The technique allows for wind speed characterization with a spatial resolution of 0.3 m on a 1 s time scale. The flow in the wind tunnel was varied in a controlled manner, such that the mean wind, ranged between 1 and 17 ms^{-1}. The AHFO measurements are compared to sonic anemometer measurements and show a high overall correlation (~~0.85-0.98~~0.94-0.99). Both the precision and accuracy of the AHFO measurements were also greater than 95% for all conditions. We conclude that the AHFO has potential to ~~be employed as an outdoor observational technique. It~~ measure wind speed and we present a method to help for choosing the heating settings of AHFO. AHFO allows for characterization of spatially varying fields of mean wind in complex terrain, such as in canopy flows or in sloping terrain. In the future, the technique could be combined with conventional Distributed Temperature Sensing (DTS) for turbulent heat flux estimation in micrometeorological/hydrological applications.

1 Introduction

This work presents the results of a wind tunnel study designed to test the novel ~~Active~~ Actively Heated Fiber-Optic (AHFO) (Sayde et al. (2015)) wind speed measurement technique in controlled airflow conditions. The primary aims of the experiment were to assess the directional sensitivity and signal-to-noise ratio of AHFO.

Wind speed is most commonly observed using in-situ point measurement techniques. As a result, the spatial distribution of field observations is limited. While it is possible to obtain distributed wind speed observations with remote sensing (e.g., Goodberlet et al. (1989)), the spatial resolution is too low for many micrometeorological applications.

Many field experiments assume Taylor's frozen flow hypothesis (Taylor (1938)) in order to estimate fluxes with similarity theory (e.g., Higgins et al. (2009); Kelly et al. (2009); Bou-Zeid et al. (2010); Patton et al. (2011)). However, similarity theory only holds for idealized homogeneous/stationary conditions, which are rarely met in practice, resulting in a model containing strong assumptions, which often leads to significant errors (Ha et al. (2007); Higgins et al. (2012); Thomas et al. (2012)). In real, non-idealized situations, even slight surface heterogeneities can lead to dramatic impacts on the spatial structure of the flow in the surface boundary layer. Further, even if perfect surface homogeneity was possible, other atmospheric (surface) conditions are often nonstationary as well (Holtslag et al. (2013)).

In the past decade, a new way to obtain spatial distributed measurements was introduced into environmental studies. ~~High-resolution~~ High spatial resolution measurements could be used to check underlying assumptions and would reduce the need for such assumptions in real-world cases. Distributed Temperature Sensing (DTS) technology measures temperature at high temporal and spatial resolution over distances of up to several kilometers by using Fiber Optic (FO) cables as sensors (Selker et al. (2006a); Selker et al. (2006b); Tyler et al. (2009)). High-end DTS can measure the temperature at a 1 s and 0.3 m resolution (Sayde et al. (2014)). The ability to report temperature at such high resolution has proven useful in many environmental studies (Selker et al. (2006a); Selker et al. (2006b); Tyler et al. (2008); Tyler et al. (2009); Steele-Dunne et al. (2010)), including atmospheric experiments (Keller et al. (2011); Petrides et al. (2011); Schilperoort et al. (2018); Higgins et al. (2018)~~);~~ ~~?~~; Izett et al. (2019)). It has also been shown that it is possible to observe air temperature and thermal structure of near-surface turbulence with DTS (Thomas et al. (2012); Euser et al. (2014); Zeeman et al. (2015), Jong et al. (2015)).

Recently, Sayde et al. (2015) ~~,~~introduced the AHFO technique as a means of performing independent explicit wind speed measurements using distributed temperature sensing (DTS) technology. The underlying concept of the proposed method is similar to that of a hotwire anemometer; however, instead of single point measurements, AFHO enables distributed measurements to be made at high spatial resolution. Instead of only passively measuring the temperature in the fiber (as is done with DTS), one segment of the cable is actively heated. The heated segment is positioned parallel to the unheated reference segment, with a small separation, in our case 0.1 m. The temperature difference between the heated and reference segment is measured, i.e., the heated fiber and the air temperature. The temperature difference between the cables depends on the energy input as well as on the wind speed of the ambient air, which determines the magnitude of the lateral heat exchange, through ~~advection of cooler ambient air~~convective heat loss. By setting up an energy balance for the heated cable, one can estimate the magnitude of this advective heat transport, which leads to an estimate of the wind speed.

Results from a field study by Sayde et al. (2015) demonstrated promising performance of the AHFO technique, but they recommended further tests on two aspects to be performed in controlled airflow conditions. First, the heat transfer model assumes the flow is normal to the axis of the fiber. Sayde et al. (2015) developed a first-order estimate of the influence of a non-normal angle of attack (the difference between the wind direction and the axis of the fiber), using a directional sensitivity equation from hotwire anemometry (Webster (1962); Hinze (1975);Perry (1982);Adrian et al. (1984)), but it needs to be tested

in a controlled setting to determine its validity. Second, Sayde et al. (2015) highlight the importance of a sufficient signal-to-noise ratio when conducting measurements. They show that the temperature difference between the heated and reference segments gives a good estimate for this ratio. The influence of the directional sensitivity and the signal-to-noise ratio on the measurement accuracy and precision is investigated and the results are used to propose a method to estimate the precision for future experiments with AHFO, hence our work will improve the possibilities for successful application of AHFO in future field experiments.

Finally, in the future it will be interesting to perform outdoor tests with AHFO in complex terrain, for both micrometeorological and hydrological applications, as AHFO gives a lot of insights in spatial varying wind fields. AHFO can be especially interesting in non-homogenous field sites, like forests, which are already studied with other DTS applications (Schilperoort et al. (2018)). Moreover, the ability to measure spatial varying wind fields can be useful for estimating sensible heat fluxes in a variety of atmosphere-vegetation-soil continuums.

An overview of the experimental setup is presented in section 2, with the accuracy and precision of the AHFO experiments presented in section 3. In section 4, a method for estimating the precision for future experiments is introduced, followed by a short note on future studies.

2 Experimental Set-Up and Methods

2.1 ~~Wind tunnel experiments~~DTS and Signal-to-Noise ratio analysis

~~We conducted a series of experiments under tightly controlled airflow conditions to improve the applicability of AHFO in experimental (field) research and to study the directional sensitivity and influence of the signal-to-noise ratio. The experiments presented were performed in a wind tunnel at Oregon State University. This wind tunnel has a closed circuit, which means the air inside is recycled. The test section of the wind tunnel has a cross-section (height by width) of 1.23 by 1.52 m, and an undisturbed horizontal section of roughly 5 to 6 m which may be used for probing. During the experiment two segments of one cable (which encloses the FOs)were placed 8 cm apart: one heated and one reference segment. For validation, an independent sonic anemometer was placed approximately 0.2 m downwind of the fibers, which measures the wind speed in 3 directions. All equipment was mounted using custom-designed support material.~~

~~a) Schematic of the wind tunnel setup and b) photograph of the experimental setup in the wind tunnel.~~

~~The angle of the fiber related to the flow, wind speed and heating rate were systematically changed. An electrical current (I) is passed through the heated cable, to create the temperature difference (ΔT, e~~Based on the backscattered signal of a laser pulse inside fiber optic cables, a Distributed Temperature Sensing (DTS) machine measures temperature along a complete fiber optic cable (Selker et al. (2006b)). ~~g., 2 C) needed to determine wind speed. By fixing the current through the stainless steel casing of the cable, the entire FO cable is heated because of the electrical resistance (R) of the stainless steel casing. The magnitude of the current needed to create a given temperature difference is dependent on the cable resistance and the wind speed, therefore the current is adjusted for each individual experiment. The amount of power applied per meter of cable, P_s (Wm^{-1}), necessary to heat the cable and to create a temperature difference, is~~ These fiber optic cables can have lengths up to

several kilometers with a spatial resolution down to 0.3 m, i.e., one DTS machine makes to thousands of near-simultaneous individual measurements. Laser pulses are sent with a fixed wavelength and most backscattered light keeps this wavelength, however some backscattered laser shifts to a shorter or longer wavelength, these frequency-shifted reflections are referred to as ~~the heating rate.~~

~~The cable was mounted at four different angles in the wind tunnel, resulting in different angles of attack, in order to gain more insights into directional sensitivity. In Figure 2b the 90° set-up is visible, however the cable was also mounted at a 45°, 30° and 15° angle, with respect to the floor of the wind tunnel (see: Figure 2a, inset) . During all set-ups, the lower part of the FO cable was fixed to the opening in the bottom of the wind tunnel, while the upper end was attached to an extruded aluminum bar that was moved over the fixed horizontal bars, to achieve the desired cableangles. To test the performance for a range of wind speeds, ten different wind speeds were tested at every angle: 1, 3, 5, 7, 9, 11, 13, 15, 16 and 17 ms^{-1} (e.g., 4x10 = 40 setups~~Raman-backscatter (Selker et al. (2006a)). By counting the backscattered photons with a longer (Stokes) and shorter (Anti-Stokes) frequency, a ratio between these two can be calculated. The strength of the Anti-Stokes signal depends on temperature, hence the ratio between the power of the Stokes and Anti-Stokes changes with temperature. This principle is used to measure the temperature along the cable. Consequently, a main source of noise in DTS data is white noise induced by the statistical variability in photon count from backscatter (optical shot noise). The ~~AHFO wind speed measurements can be calibrated by comparing the AHFO wind speed to a reference sonic anemometer. The wind speed in~~ white noise can be reduced by averaging over multiple measurements in either space or time, assuming the observed temperature is/stays (relatively) constant van de Giesen et al. (2012).

A sufficiently high signal-to-noise ratio is essential for measurement precision with DTS. In Sayde et al. (2015) it is shown that the signal-to-noise ratio can be described as: $(T_s - T_f)/T_{error}$, where T_s and T_f are the temperature (in K) of the ~~wind tunnel was fixed at a constant value to create a steady state flow. In field experiments the wind speed will vary, and the temperature difference will fluctuate accordingly if the current is fixed. For all angles and every wind speed, three temperature differences were applied in order to quantify the importance of the~~ heated cable segment and (unheated) reference segment (i.e., air temperature). Hence the signal-to-noise ~~ratio. The current was fixed to create a temperature difference (ΔT) of 2, 4~~ ratio is related to the ΔT (= $T_s - T_f$) and ~~6 °C between the heated and reference cable.In total, 120 (4 x 10 x 3)trials were conducted with the different parameters, each with a minimum duration of 10 minutes.~~

~~The cable mounted in the wind tunnel consisted of a 1.34 mm outer diameter stainless steel casing that enclosed four multi-mode FOs with a diameter of 250 µm (Figure 3) . Only two FOs were used and these were spliced at the end of the cable to create a duplexed FO, which results in double measurements (Hausner et al., 2011). The FOs were connected to a Silixa Ultima DTS machine (Ultima S, 2 km range, Silixa, London, UK) outside the wind tunnel.~~

~~Cross-section of the FO cable~~

~~One cable segment was heated. The stainless steel casing was connected to a power controller (MicroFUSION uF1HXTA0-32-P1000-F04 by 12 AWG cables (3.31 mm^2),~~ the measurement error of the DTS, T_{error} (in this study at a 1 s sample resolution). A large ΔT is obviously desirable, however, ΔT cannot be increased infinitely. The power controller can only deliver a limited amount of power to heat the ~~cable in a controlled way. Heating rates varying from 0.5-10 Wm^{-1} were used to create temperature differences~~

to a fixed level, either 2, 4 and 6 °C, depending on the setup. The electrical resistance per meter of stainless steel casing (R_s) is 1.67 fiber, which is especially relevant for the heating of long lengths of FO cable (Ωm^{-1}) and is constant along the length. For the length of a cable segment (B, (m)), $R = R_s B$, where R (Ω) is the total resistance of a cable segment. The same holds for $P = P_s B$, where P (W) is the total power input for a cable segment.The heating rate for a cable segment (Wm^{-1}) was controlled by fixing the current, I (A), during experiments, as the current is also constant over the entire heated segment, the heating rate is as well. Hence, the known relation $P = I^2 R$ (W), or in this specific case the heating rate is $P_s = I^2 R_s$ (Wm^{-1}) per meter of cable segment.

For calibration and validation of the DTS data, approximately 6 m of the FO cables was placed in a well-mixed ambient bath to calibrate the DTS temperature according to the method described by Hausner et al. (2011). The temperature was verified with one probe (RBRsolo^2 T, RBR Ltd., Ottawa, Ontario, Canada). A circulating aquarium pump was placed inside the bath, to prevent stratification.

Temperatures along the FOs were sampled at 0.125 m resolution with a sampling rate of 1 Hz. The FOs were deployed in a double-ended configuration, however the data was acquired and treated as two separated single-ended channels of data. Splices between ends of fiber optic cables are known to create an additional loss in signal, i.e., local higher attenuation (Tyler et al. (2009); van de Giesen et al. (2012)), this loss is normally independent of the direction. However, in processing of the raw DTS data it was found that the loss over the splice was not the same in both directions. Due to this asymmetrical structure of the splice loss, only the data of one channel was used to ensure the quality of the results, as this channel showed a regular splice loss.

To be able to test the accuracy of the DTS i.e. several hundreds of meters of FO cable). Also the creation of larger temperature differences means the importance of other ways of transferring energy changes (e.g., free convection, radiation and diffusion). The effect of ΔT is investigated by using three temperature differences during the experiment. The effect of the signal-to-noise ratio is quantified, and an equation to estimate the precision is presented. The measurement precision is an indication of the variability of wind speed measurements independently, wind speed was sampled at 10 Hz using a sonic anemometer (IRGASON+EC100 and CR3000, Campbell Scientific, Logan, UT,USA).The sonic anemometer was mounted approximately 0.2 m behind the fiber optic cables, in the middle of the wind tunnel.As the FOs are very thin, it is assumed that these do not significantly disturb the measurement of the sonic volume (particularly at larger averaging times(e.g., RMSD), as opposed to accuracy which describes a systematic measurement error for which van be compensated (in our case expressed by the bias).

2.2 Determination of Wind Speed

2.2.1 Determination Original determination of Wind Speed by Sayde et al. (2015)

An energy balance is used to quantify the advective energy transport heat dissipation from the heated cablesection, and therefore estimate the wind speed with DTS. The advective cooling can be converted to wind speed, because it is a function of wind

speed and the temperature difference between the heated and unheated segments. The full energy balance (in W) for a cable segment volume of length, B, is given by Sayde et al. (2015), and schematically shown in Figure 1:

$$c_s \rho_v V \frac{\mathrm{d}T_s}{\mathrm{d}t} = P_s B + (\bar{S}_b + \bar{S}_d + \alpha_s \bar{S}_t)(1-\alpha_f) 2r\pi B + (\bar{L}_\downarrow + \bar{L}_\uparrow)\epsilon 2r\pi B - \epsilon\sigma T_s^4 2r\pi B - h(T_s - T_f)2r\pi B \quad (1)$$

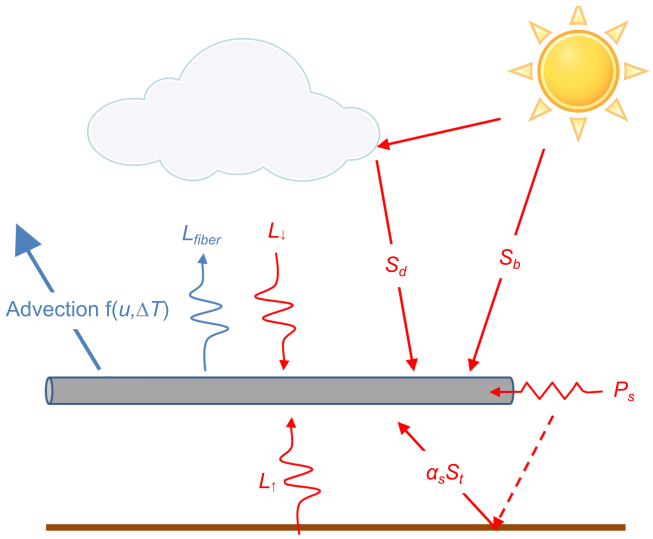

Figure 1. Schematization of the energy balance, based on Sayde et al. (2015)

Where, r is the radius of the cable ($6.7 \cdot 10^{-4}$ m in our setup); V is the volume of the cable segment ($\pi r^2 B$, in m^3), c_s is the specific heat capacity of the FO cable (502 $Jkg^{-1}K^{-1}$) and ρ_v is the FO cable density (800 kgm^{-3}). P_s is the heating rate per meter of cable (in Wm^{-1}); and B is the length of a cable segment (in m). $\bar{S}_b, \bar{S}_d$ and $\alpha_s \bar{S}_t$ (in Wm^{-2}) are the mean direct, diffuse and reflected short wave radiation fluxes, respectively, with α_s being the surface albedo of the ground; and α_f is the FO cable optic surface albedo. $\bar{L}_\downarrow + \bar{L}_\uparrow$ (in Wm^{-2}) are the average downward and upward longwave radiation fluxes, respectively; and ϵ is the FO cable surface emissivity. Based on the kind of stainless steel, emissivity values can range from 0.3 to 0.7 (Baldwin and Lovell-Smith (1992)); however, we assume a value of 0.5 (Madhusudana (2000)). σ is the Stefan-Boltzmann constant, $5.67 \cdot 10^{-8}$ (Wm^{-2} K^{-4}); and $\epsilon\sigma T_s^4$ is the outgoing longwave radiation of the fiber, i.e., L_{fiber}; ~~T_s and T_f are the temperature (in K) of the heated cablesegment and (unheated) reference segment (i. e., air temperature), respectively. Finally, h is the~~ h is the advective heat transfer coefficient ($Wm^{-2}K^{-1}$).

Simplification

The energy balance is simplified, by dividing Eq. 1 by $2r\pi B$, which is equal to the surface area of the FO cable. The energy balance now no longer depends on B, meaning the length of FO segment does not need to be defined. The proposed final energy balance by Sayde et al. (2015) is as follows and in Wm^{-2}:

$$\frac{c_s \rho r}{2}\frac{dT_s}{dt} = \frac{P_s}{2\pi r} + (\bar{S}_b + \bar{S}_d + \alpha_s \bar{S}_t)(1-\alpha_f) + (\bar{L}_\downarrow + \bar{L}_\uparrow)\epsilon - \epsilon\sigma T_s^4 - h(T_s - T_f) \quad (2)$$

where, ρ is the FO cable density per meter of cable segment: 4.5 x 10^{-3} kgm^{-1}.

Advective heat transfer coefficient

The advective heat transfer coefficient ~~(in~~ h ($Wm^{-2}K^{-1}$) ~~. By~~ can by means of the dimensionless Nusselt (Nu), Prandtl (Pr), and Reynolds (Re) numbers ~~, h can~~ be expressed as function of the wind speed, ~~$h = f(u_n)$. Nu,~~ $h = f(u_n)$. The Nusselt number is the ratio between the advective and conductive heat transfer, where the Nusselt number can be written as follows ~~,~~(Žukauskas (1972)):

$$\mathrm{Nu} = \frac{h d_s}{K_a} = C\mathrm{Re}^m \mathrm{Pr}^n \left(\frac{\mathrm{Pr}}{\mathrm{Pr}_s}\right)^{\frac{1}{4}} \quad (3)$$

with,

$$\mathrm{Nu} = C\mathrm{Re}^m \mathrm{Pr}^n \left(\frac{\mathrm{Pr}}{\mathrm{Pr}_s}\right)^{\frac{1}{4}}$$

$$\mathrm{Re} = \frac{u_n d_s}{\upsilon_a} \quad (4)$$

d_s is the fibers characteristic length ($2r$); K_a is the thermal conductivity of air and υ_a the kinematic viscosity of air, respectively 0.0255 $Wm^{-1}K^{-1}$ and 1.5 x 10^{-5} m^2s^{-1} (Tsilingiris (2008)). K_a and υ_a are assumed to be constant, due to the controlled conditions in the wind tunnel, but in field experiments this should be included as a variable, as K_a and υ_a are temperature and relative humidity depend (Tsilingiris (2008)). C, m and n are empirical constants related to forced advection of heat by air movement. In Sayde et al. (2015), C, m and n values of 0.51, 0.5 and 0.37 are set, based on (Žukauskas (1972)). Pr is the Prandtl number and can be seen as the ratio between kinematic viscosity and thermal diffusivity, which, we assume Pr to be constant (0.72) for our range of temperatures (12-35 ~~°C~~K), as in Tsilingiris (2008), with Pr_s (the Prandtl number for the heated fiber segment), assumed to be the same as Pr, due to the small temperature differences (max. 6 ~~°C~~K). Lastly, Re is the Reynolds number which is used to determine the flow regime of the air along the fiber segments, i.e., Re expresses if the flow regime is laminar or turbulent. Combining Eq. 3-4 yields:

$$h = C d^{m-1} \mathrm{Pr}^n \left(\frac{\mathrm{Pr}}{\mathrm{Pr}_s}\right)^{\frac{1}{4}} K_a \upsilon_a^{-m} u_n^m \quad (5)$$

The determination of the Nusselt number (Eq. ??3) is only valid in the following ranges of Re (40-1000) and Pr (0.7-500). Re can be a limitation for higher wind speeds, especially when the diameter of the fiber is large, in our case wind speeds higher than approximately 11 ms^{-1} would be out of range. In the derivation of the energy balance (1), there is assumed to be no free convection, induced by heating of the air close to the cable, and no conduction of heat in the axial direction of the FO cable. It is also assumed there is no radiative exchange between objects close and parallel to the heated fiber, i.e., dispersion of heat from the heated cable to the reference cable is assumed to be negligible. Furthermore, a flow directed normal to the axis of FO cable is assumed by the proposed energy balance, i.e., for flow directed in a different angle, compensation is necessary to accurately estimate the wind speed.

~~Finally, the energy balance is simplified, by dividing Eq. 1 by $2r\pi B$, which is equal to the surface area of the FO cable. The energy balance now no longer depends on B, meaning the length of FO segment does not need to be defined. The proposed final energy balance by Sayde et al. (2015) is as follows and in Wm^{-2}:~~

~~$$\frac{c_s \rho r}{2}\frac{\mathrm{d}T_s}{\mathrm{d}t} = \frac{P_s}{2\pi r} + (\bar{S}_b + \bar{S}_d + \alpha_s \bar{S}_t)(1-\alpha_f) + (\bar{L}_\downarrow + \bar{L}_\uparrow)\epsilon - \epsilon\sigma T_s^4 - h(T_s - T_f)$$~~

~~where, ρ is the FO cable density per meter of cable segment: 4.5 x 10^{-3} kgm^{-1}.~~

2.2.2 ~~Proposed~~ Revised simplified determination of Wind Speed

Due to the setup inside the wind tunnel, as opposed to outdoor conditions, some simplifications can be made. The short wave radiation can be neglected because it is an indoor experiment (no sunlight). Furthermore, we assume that there is a uniform temperature inside the wind tunnel, due to the enclosed conditions. This means the incoming radiation is dependent on the air temperature, T_f. Assuming incoming $(\bar{L}_\downarrow + \bar{L}_\uparrow)$ to be black body radiation (i.e., $L_{in} = \sigma T_s^4$), the net longwave radiation loss for the fiber can be simplified accordingly by merging the incoming longwave and outgoing longwave radiation as:

$$(\bar{L}_\downarrow + \bar{L}_\uparrow)\epsilon - \epsilon\sigma T_s^4 \approx -\epsilon\sigma(T_s^4 - T_f^4) \tag{6}$$

One more additional change is made, based on our results obtained during testing of the performance of the AHFO technique. In processing of the obtained wind tunnel data it was found that by using the calculation of the Nusselt number from Žukauskas (1972), Eq. 3, a $\sim 20\%$ additional bias in calculating the wind speed was created. By using a more recent version for calculating the empirical Nusselt number (Cengel and Ghajar (2014)), the bias in our study is reduced to $\sim 5\%$ Therefore, Eq. 7 is proposed to calculate the Nusselt number, where the constants C, m and n are still used; however, with the values from Table 7-1 ($C = 0.683, m = 0.466$ and $n = 1/3$) in Cengel and Ghajar (2014), rather than those in Žukauskas (1972). Next to the improved fit, the range of Re over which the equation is valid is much wider (40-4000 compared with 40-1000), and therefore more applicable in future AHFO experiments.

$$\mathrm{Nu} = C\mathrm{Re}^m\mathrm{Pr}^n = 0.683\mathrm{Re}^{0.466}\mathrm{Pr}^{1/3} \tag{7}$$

Consequently, the expression of h changes as well.

$$h = Cd^{m-1}\mathrm{Pr}^{n}K_a\upsilon_a^{-m}u_n^{m} \tag{8}$$

With the long- and short-wave radiation simplifications, the ~~simplified~~ energy balance becomes:

$$\frac{c_s\rho r}{2}\frac{\mathrm{d}T_s}{\mathrm{d}t} = \frac{P_s}{2\pi r} - \epsilon\sigma(T_s^4 - T_f^4) - h(T_s - T_f) \tag{9}$$

By substituting the expression for h (Eq. 8), we can rearrange Eq. 9 to obtain an expression for wind speed. Eq. 10 will be used to estimate the wind speed (u_N) in our wind tunnel study.

$$u_N = \left(\frac{0.5P_s\pi^{-1}r^{-1} - \epsilon\sigma(T_s^4 - T_f^4) - 0.5c_p\rho r\frac{\mathrm{d}T_s}{\mathrm{d}t}}{Cd^{m-1}\mathrm{Pr}^{n}K_a\upsilon_a^{-m}(T_s - T_f)}\right)^{1/m} \tag{10}$$

2.3 ~~Directional Sensitivity analysis~~Wind tunnel experiments

We conducted a series of experiments under tightly controlled airflow conditions to improve the applicability of AHFO in experimental (field) research and to study the directional sensitivity and influence of the signal-to-noise ratio. The experiments presented were performed in a wind tunnel at Oregon State University. This wind tunnel has a closed circuit, which means the air inside is recycled. The test section of the wind tunnel has a cross-section (height by width) of 1.23 by 1.52 m, and an undisturbed horizontal section of roughly 5 to 6 m which may be used for probing. During the experiment two segments of one cable (which encloses the FOs) were placed 8 cm apart: one heated and one reference segment. For validation, an independent sonic anemometer was placed approximately 0.2 m downwind of the fibers, which measures the wind speed in 3 directions. All equipment was mounted using custom-designed support material.

The angle of the fiber related to the flow, wind speed and heating rate were systematically changed. An electrical current (I) is passed through the heated cable, to create the temperature difference that is necessary to measure wind speed (ΔT, e.g., 2 K). By fixing the current through the stainless steel casing of the cable, the entire FO cable is heated because of the electrical resistance (R) of the stainless steel casing. The magnitude of the current needed to create a given temperature difference is dependent on the cable resistance and the wind speed, therefore the current is adjusted for each individual experiment. The amount of power applied per meter of cable, P_s (Wm^{-1}), necessary to heat the cable and to create a temperature difference, is referred to as the heating rate.

The cable was mounted at four different angles in the wind tunnel, resulting in different angles of attack to mean flow direction, in order to gain more insights into directional sensitivity. In Figure 2b the 90° set-up is visible, however the cable was also mounted at a 45°, 30° and 15° angle, with respect to the floor of the wind tunnel (see: Figure 2a, inset). During all set-ups, the lower part of the FO cable was fixed to the opening in the bottom of the wind tunnel, while the upper end was attached to an extruded aluminum bar that was moved over the fixed horizontal bars, to achieve the desired cable angles. To

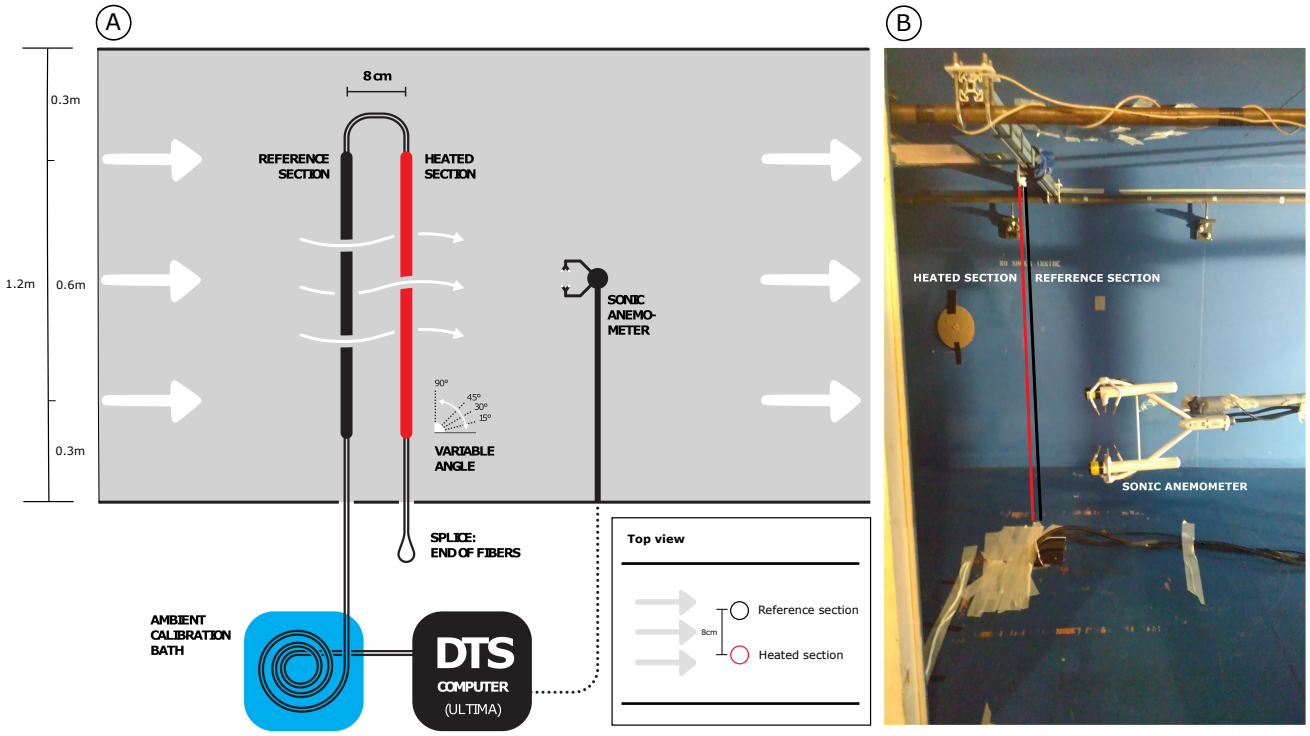

Figure 2. a) Schematic of the wind tunnel setup and b) photograph of the experimental setup in the wind tunnel.

test the performance for a range of wind speeds, ten different wind speeds were tested at every angle: 1, 3, 5, 7, 9, 11, 13, 15, 16 and 17 ms^{-1} (e.g., 4x10 = 40 setups). The AHFO wind speed measurements can be calibrated by comparing the AHFO wind speed to a reference sonic anemometer. The wind speed in the wind tunnel was fixed at a constant value to create a stable, non-turbulent, steady state flow (Appendix B). In field experiments the wind speed will vary, and the temperature difference will fluctuate accordingly if the current is fixed. In order to quantify the importance of the signal-to-noise ratio for all possible combinations of angles and wind speed (4 x 10), three temperature differences were applied. The current was fixed to create a temperature difference (ΔT) of 2, 4 and 6 K between the heated and reference cable. In total, 120 (4 x 10 x 3) trials were conducted with the different parameters, each with a minimum duration of 10 minutes.

The cable mounted in the wind tunnel consisted of a 1.34 mm outer diameter stainless steel casing that enclosed four multi-mode FOs with a diameter of 250 µm (Figure 3). Only two FOs were used and these were spliced at the end of the cable to create a duplexed FO, which results in double measurements for each measuring point along the FO (Hausner et al., 2011). The FOs were connected to a Silixa Ultima DTS machine (Ultima S, 2 km range, Silixa, London, UK) outside the wind tunnel.

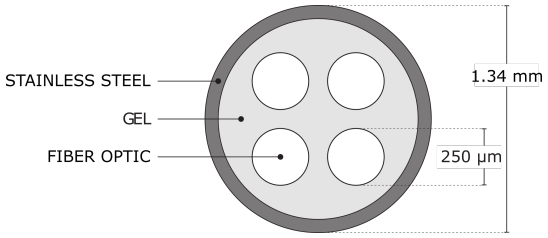

Figure 3. Cross-section of the FO cable

One cable segment was heated by connecting the stainless steel casing to a power controller (MicroFUSION uF1HXTA0-32-P1000-F040 by 12 AWG (copper) cables (3.31 mm^2), to heat the cable in a controlled way. Heating rates varying from 0.5-10 Wm^{-1} were used to create temperature differences to a fixed level depending on the setup. The electrical resistance per meter of stainless steel casing (R_s) is 1.67 (Ωm^{-1}) and is constant along the length. For the length of a cable segment (B, (m)), $R = R_s B$, where R (Ω) is the total resistance of a cable segment. The same holds for $P = P_s B$, where P (W) is the total power input for a cable segment. The heating rate for a cable segment (Wm^{-1}) was controlled by fixing the current, I (A), during experiments, as the current is also constant over the entire heated segment, the heating rate is as well. Hence, the known relation $P = I^2 R$ (W), or in this specific case the heating rate is $P_s = I^2 R_s$ (Wm^{-1}) per meter of cable segment.

For calibration and validation of the DTS data, approximately 6 m of the FO cables was placed in a well-mixed ambient bath to calibrate the DTS temperature according to the method described by Hausner et al. (2011). The temperature was verified with one probe (RBRsolo^2 T, RBR Ltd., Ottawa, Ontario, Canada). A circulating aquarium pump was placed inside the bath, to prevent stratification.

Temperatures along the FOs were sampled at 0.125 m resolution with a sampling rate of 1 Hz. The FOs were deployed in a double-ended configuration, however the data was acquired and treated as two separated single-ended channels of data. Splices between ends of fiber optic cables are known to create an additional loss in signal, i.e., local higher attenuation (Tyler et al. (2009); van de Giesen et al. (2012)), this loss is normally independent of the direction. However, in processing of the raw DTS data it was found that the loss over the splice was not the same in both directions. Due to this asymmetrical structure of the splice loss, only the data of one channel was used to ensure the quality of the results, as this channel showed a regular splice loss.

In our study we use the advantage of averaging over time and space, to reduce (white) noise in the DTS measurements (van de Giesen et al. (2012); Selker et al. (2006b)). For clarity we therefore introduce three parameters: n_{time}, n_{space} and n, where n_{time} is the amount of measurements averaged over time and n_{space} is the amount of measurements averaged over space and n the total amount of measurements over time and space and can be expressed as: $n = n_{time} \times n_{space}$. In the machine specifications it is given that the sample resolution is $x_{sample} = 0.125$m, but the highest actual spatial resolution is 0.3m, indicating and $n_{space} \geq 2$. In this paper we will first work with $n_{space} = 10$ and finally we will propose an equation (See later Eq. 22) which is a function of $n_{space} = 1$. This is done, because we want to estimate an unique constant (C_{DTS})

independent of the DTS machine and the settings, which is expected to be more representative if the amount of (white) noise is reduced by averaging.

To be able to test the accuracy of the DTS wind speed measurements independently, wind speed was sampled at 10 Hz using a sonic anemometer (IRGASON+EC100 and CR3000, Campbell Scientific, Logan, UT,USA). The sonic anemometer was mounted approximately 0.2 m behind the fiber optic cables, in the middle of the wind tunnel. As the FOs are very thin, it is assumed that these do not significantly disturb the measurement of the sonic volume (particularly at larger averaging times).

2.4 Directional sensitivity analysis

Equation 10 is derived for flows normal to axis of the cable (as in Figure 2b). However, in reality the wind will not always have a 90° angle compared to the axis of the cable, especially in outside atmospheric experiments. For angles smaller than 90° the wind speed will be underestimated, as the advective heat transfer is less efficient. To be able to still determine the wind speed for all angles of attack, Sayde et al. (2015) adjusted the wind speed obtained in Eq. 10 using a geometric correction from hotwire anemometry (e.g., Adrian et al. (1984)) to get the true wind speed (u_{DTS}):

$$u_{DTS} = \sqrt{\frac{u_N^2}{\cos^2(\varphi - 90°) + k^2 \sin^2(\varphi - 90°)}} \sqrt{\frac{u_N^2}{\cos^2(\varphi - 90°) + k_{ds}^2 \sin^2(\varphi - 90°)}} \tag{11}$$

~~k~~ k_{ds} is the directional sensitivity and φ is the angle of attack of the wind with respect to the axis of the cable, ranging from 0° to 90°. ~~However, during~~

3 Results and Discussion

3.1 Proposed directional sensitivity equation

During analysis of the wind tunnel data it was found that Eq. 11 was not giving satisfying results (e.g., a 22% bias between the 90° and 15° angle). In Adrian et al. (1984) it is shown that in hotwire anemometry a variety of theoretical and empirical formulas have been proposed in the past, in order to account for directional sensitivity. Alternatively, using the formula suggested by Bruun (1971) gives more satisfying results, diminishing the bias between the 90° and 15° angle to only ~~5~~4%. This is shown in Figure 4.

Therefore, Eq. 12 is used to account for directional sensitivity in our study, with the scaling exponent, m_1, able to be optimized during calibration of the AHFO measurements. The value for m_1 obtained during calibration of our set up was 1.05.

$$u_{DTS} = \frac{u_N}{\cos(\varphi - 90°)^{m_1}} \tag{12}$$

3.2 ~~DTS~~ Accuracy and ~~Signal-to-Noise ratio analysis~~precision

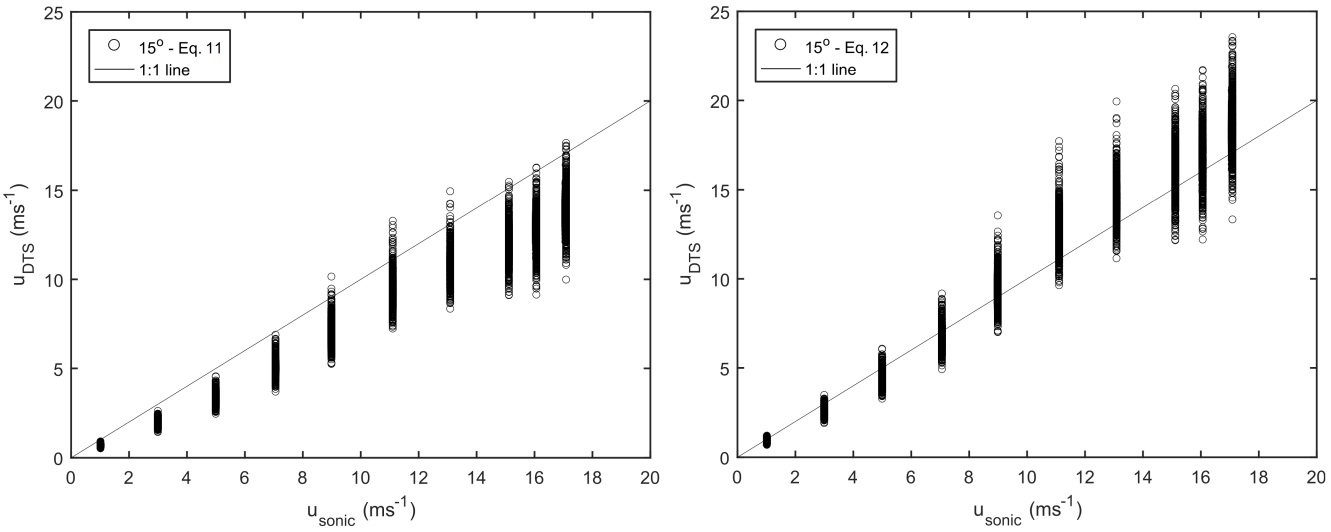

Figure 4. ~~a) 90° angle (no correction), b)~~ Directional sensitivity shown for 15° angle~~corrected with~~ , original Eq. 11 ~~., c~~(a) ~~15° angle corrected with~~ and proposed Eq. 12 (b).

~~Based on the backscattered signal of a laser pulse inside fiber optic cables, a Distributed Temperature Sensing (DTS) machine measures temperature along a complete fiber optic cable (Selker et al. (2006b)). These fiber optic cables can have lengths up to several kilometers with a spatial resolution down to 0.3 m, i.e., one DTS machine makes to thousands of near-simultaneous individual measurements . Laser pulses are sent with a fixed wavelength and most backscattered light keeps this wavelength, however some backscattered laser shifts to a shorter or longer wavelength, these frequency-shifted reflections are referred to as Raman-backscatter (Selker et al. (2006a)). By counting the backscattered photons with a longer (Stokes) and shorter (Anti-Stokes) frequency, a ratio between these two can be calculated. The strength of the Anti-Stokes signal depends on temperature, hence the ratio between the power of the Stokes and Anti-Stokes changes with temperature. This principle is used to measure the temperature along the cable. Consequently, a main source of noise in DTS data is white noise induced by the statistical variability in photon count from backscatter (optical shot noise). Furtherr sources of noise include Johnson-Nyquist noise.~~

~~A sufficiently high signal-to-noise ratio is essential for measurement precision with DTS. In Sayde et al. (2015) it is shown that the signal-to-noise ratio can be described as: $(T_s - T_f)/\sigma_T$. Hence the signal-to-noise ratio is related to the ΔT ($T_s - T_f$) and the measurement error of the DTS, σ_T (in this study at a 1 s sample resolution), which can be assumed constant in a lab experiment. A large ΔT is obviously desirable, however, ΔT cannot be increased infinitely. The power controller can only deliver a limited amount of power to heat the fiber, which is especially relevant for the heating of long lengths of FO cable (i.e. several hundreds of meters of FO cable). Also the creation of larger temperature differences means the importance of other modes of energy transfer changes. To find realistic solutions, the effect of ΔT is investigated by using three temperature differences during the experiment. The effect of the signal-to-noise ratio is quantified, and an equation to estimate the precision~~

~~is presented. The precision is an indication of the variability of wind speed (e.g., RMSD), as opposed to accuracy which describes a systematic measurement error that can be removed through calibration (e.g., a bias).~~

4 ~~Results~~

~~The accuracy and precision of the DTS wind speed calculations is given~~ In Figure 4b the AHFO wind speed measurements are compared to the velocity measured with the sonic anemometer. The comparison for all angles can be found in Figures A1 and A2~~, where the velocity calculated using AHFO (calculated by Eq. 10 and 12) is compared with the velocity measured from the sonic anemometer. The temperatures~~ . The wind speeds measured with AHFO are ~~spatially averaged over~~ calculated using 10 ~~measurements (~~temperature differences (duplex setup with 2 ~~fibers, each with~~ $\times$ 5 heated and reference measurements), i.e., for the 90° setup this is equivalent to a height of $\sim$ ~~0.9~~ 0.675 m in the wind tunnel. ~~Only the temperatures~~ For each angle of attack only the 5 temperatures differences ($\times$2 because of duplexing) from the middle of the wind tunnel are used, to prevent using ~~data~~ AHFO wind speed measurements with side/boundary effects. We investigated the consequences of extending the spatial range and found there is limited difference between these measurements (see Table C1). During this extended spatial range analysis we found out part of the 90° data of the duplexed cable contained additional noise which decreased the accuracy, and therefore we decided to take only 5 $\times$ 1 temperature differences for the 90° calculations.

Figure A1 shows the 1 s sample rate DTS data against the 1 s average sonic anemometer data, for the four different angles of attack. Figure A2 shows the same dataset, but temporally averaged over 30 s, and for all angles. A clear improvement of the precision is visible when temporal averaging is performed. Even though the directional sensitivity formula is not yet fully calibrated, the bias is negligible, with coefficients of determination ranging from 0.85-0.98. Finally, as expected, the wind speed measurement are less accurate when the wind speed angle is smaller.

~~Comparison of AHFO and sonic anemometer wind speed at a 1 s temporal resolution, for the four different angles of attack. a) 90°, b) 45°, c) 30°, and d) 15°~~

~~Comparison of AHFO and sonic anemometer wind speed averaged over 30 s for all angles of attack.~~

To get more insight in the quality of the results, a dimensionless analysis is performed. In Figure 5, the non-dimensional wind speed accuracy for the whole wind tunnel experiment is shown. For all combinations (120 individual cases of varying wind speed (u_j), angle and ΔT), the accuracy is calculated according to Eq. 13. ~~The accuracy is then averaged over wind speed~~ σ_a is a function of the averaging time, which is defined as $n_{time} = t_{avg}/t_{sample}$, where t_{avg} can only be a integer which is a multiple of t_{sample}. σ_a is also a function of spatial averaging, which is defined as $n_{space} = x_{avg}/x_{sample}$, where x_{avg} can only be a integer which is a multiple of x_{sample}. In Figure 5 the accuracy is averaged over all wind speeds for each ΔT and angle combination~~in Figure 5, indicating the size of the bias by σ_a~~, with $n_{space} = 10$ and n_{time} varying from 1 to 30, resulting

in 12 values for each time resolution, which can be written as: $\sigma_a(\bar{u}_j, n_{space} = 10, n_{time} = 1,5,10,15,20,25,30)$. Where $\bar{u}_j$ is the average over all individual measurements (i) of a specific wind speed u_j , where $j = 1 - 17ms^{-1}$.

$$\sigma_a(u_j, n_{space}, n_{time}) = \frac{\bar{u}_{DTS} - \bar{u}_{sonic}}{\bar{u}_{sonic}} \frac{\bar{u}_{DTS}(j) - \bar{u}_{sonic}(j)}{\bar{u}_{sonic}(j)} \tag{13}$$

For the ~~whole uncalibrated~~ data set, the maximum σ_a is ~~5~~$\pm$ 3%, which is promising for future applications. The ~~90° angle~~ $\Delta T = 6K$ should be the best performing ~~angle, however it is maximal overestimating with 5%, which is probably~~ heating setting, however this is not always the case and there is fluctuations between the heating settings, which could be due to neglecting small energy losses, like free convection due to heating of air close to the heated cable (Sayde et al. (2015)), which is temperature dependent. With such an energy loss included, the bias of each angle ~~will change. As a flow directed normal to the axis of FO cable is assumed by the proposed energy balance, it is better to compare the other angles to the 90° angle instead of 0 bias. Doing this, it can been seen that the directional sensitivity formula is not yet optimally calibrated (e.g., the 5% difference between the 90° and 15° angle biases). This kind of error is not uncommon and in accordance with previous hotwire anemometry work, especially with small angles of attack (Adrian et al. (1984)).~~ might change. Nevertheless, the bias is fairly constant with increasing averaging time, which means extensive calibration can probably increase the accuracy.

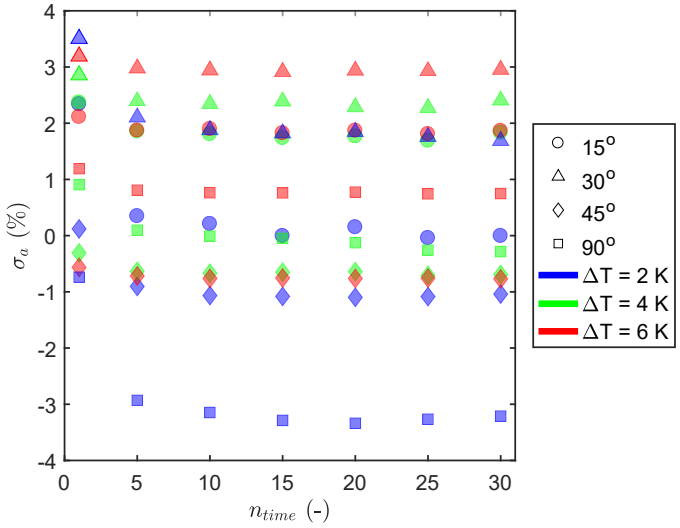

Figure 5. Bias in AHFO wind speed as a function of averaging period for different angles of attack, and different fiber heating.

While the accuracy (bias) remains constant over the averaging period, the relative precision, σ_p ~~increases~~ improves significantly (Fig. 6). The precision is calculated for all 120 ΔT, angle and wind speed ~~combination,~~ combinations (u_j, where $j = 1 - 17ms^{-1}$)), using Eq. 14. ~~To be able to present the precision clearly, the precision is averaged over wind speed for all ΔT and angle combinations in Figure 6:~~

$$\sigma_p = \frac{\text{RMSD}}{\bar{u}} = \frac{\sqrt{\sum\left(\left(u_{sonic}(i)-\bar{u}_{sonic}\right)-\left(u_{DTS}(i)-\bar{u}_{DTS}\right)\right)^2}}{\bar{u}_{sonic}}$$

$$\sigma_p(u_j, n_{space}, n_{time}) = \frac{\text{RMSD}}{\bar{u}_j} = \frac{\sqrt{\sum\left(\left(u_{sonic}(i,j)-\bar{u}_{sonic}(j)\right)-\left(u_{DTS}(i,j)-\bar{u}_{DTS}(j)\right)\right)^2 \frac{1}{n(i)}}}{\bar{u}_{sonic}(j)} \quad (14)$$

Similar to the accuracy, the precision, σ_p, is a function of the averaging time, which is again defined as $n_{time} = t_{avg}/t_{sample}$, where t_{avg} can only be a integer which is a multiple of t_{sample}. The precision, σ_p is also a function of spatial averaging, which is also here defined as $n_{space} = x_{avg}/x_{sample}$, where x_{avg} can only be a integer which is a multiple of x_{sample}.

While calculating the precision of u_{DTS}, the natural variability of the wind is excluded, by assuming the sonic anemometer is able to capture ~~this~~the natural variability and assuming the sonic anemometer measurements have a negligible instrument variability in comparison to the AHFO measurements. As a result, the variability of the DTS machine u_{DTS} estimates are obtained. For each of the 120 combinations, ~~u_{sonic} and u_{DTS}~~ $\bar{u}_{sonic}(j)$ and $\bar{u}_{DTS}(j)$ are the average wind speeds for ~~a given combination. $u_{sonic}(i)$ and $u_{DTS}(i)$~~ an u_j. $u_{sonic}(i,j)$ and $u_{DTS}(i,j)$ are single measurements ~~during this combination~~for an u_j.

~~The precision increases~~ To be able to present the precision clearly, the precision is averaged over wind speed for all ΔT and angle combinations in Figure 6, with n_{space}=10 and n_{time} varying from 1 to 30, resulting in 12 values for each time resolution, which can be written as Eq. 15, with $n_{space} = 10$ and $n_{time} = 1, 5, 10, 15, 20, 25, 30$:

$$\sigma_p = f(\bar{u}_j, n_{space}, n_{time}) \quad (15)$$

The precision improves to a σ_p less than 5% by averaging over time. Improvement by averaging is expected due to the reduction of noise (van de Giesen et al. (2012)). As mentioned, the main source of noise in DTS data is white noise, this explains the visible improvement of the precision by $\frac{1}{\sqrt{n}}$, as signal averaging is applied, where n is the amount of measurements (Selker et al. (2006b); Kaiser and Knight (1979)). Hence, in this paper n is expressed as $n_{space} \times n_{time}$, the amount of measurements in the time and space domain.

4 ~~Discussion~~

3.1 Normalized precision

In order to remove the influence of different settings (such as the choice of ΔT) and determine a general prediction of precision in future experiments, we normalize the precision. First, the precision is normalized to ΔT (Figure 7a), by multiplying Eq. 15

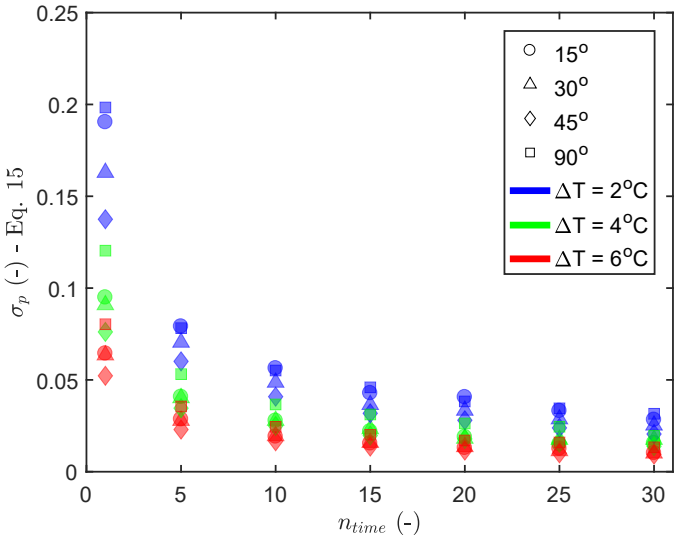

Figure 6. Precision of the AHFO wind speed measurements as a function of averaging period.

by $\frac{\Delta T}{T_{error}}$ ~~.~~, which can be written as Eq. 16.

$$\sigma_p = f(\bar{u}_j, n_{space}, n_{time}) \cdot \frac{\Delta T}{T_{error}} \tag{16}$$

As a results, $\frac{1}{\sqrt{n}}$ dependence becomes even more clear, as shown by the black solid line showing ~~$\frac{\gamma}{\sqrt{n}}$, where γ is σ_p at a 1 s temporal, and 10 measurement spatial, resolution.~~ $\frac{\bar{\sigma}_p}{\sqrt{n_{time}}} \times \frac{\Delta T}{T_{error}}$, where $\bar{\sigma}_p$ is the average of Eq.15, with $n_{space} = 10$ and n_{time}=1. Second, the precision is also normalized to the $\frac{1}{\sqrt{n}}$ behavior, by multiplying Eq. 16 by $\sqrt{\frac{t_{avg}}{t_{sample}}}$ ~~. Where,~~, resulting in Eq. 17.

$$\sigma_p = f(\bar{u}_j, n_{space}, n_{time}) \cdot \frac{\Delta T}{T_{error}} \sqrt{\frac{t_{avg}}{t_{sample}}} \tag{17}$$

T_{error} and t_{sample} are given constants which depend on the performance of the DTS, in this case $T_{error} = 0.25$ K and $t_{sample} = 1$ s, according to the factory specifications. It appears that the precision by taking the average can be condensed in ~~a~~ one number, 1.6, which we denote by the symbol C_{int} (Figure 7b). Intermediate constant C_{int} can be defined as, Eq. 18, with $n_{space} = 10$:

$$C_{int} = \gamma \frac{\Delta T}{T_{error}} \sqrt{\frac{t_{avg}}{t_{sample}}} \overline{f(\bar{u}_j, n_{space}, n_{time}) \cdot \frac{\Delta T}{T_{error}} \sqrt{n_{time}}} = 1.6 \tag{18}$$

Finally, a final constant for a 1 s and ~~0.3~~ 0.125 m resolution is desired, as this ~~this is the~~ is the sampling resolution and the starting point before any averaging takes place. Doing so, Eq. 22 can be used for different kinds of DTS machines, also when

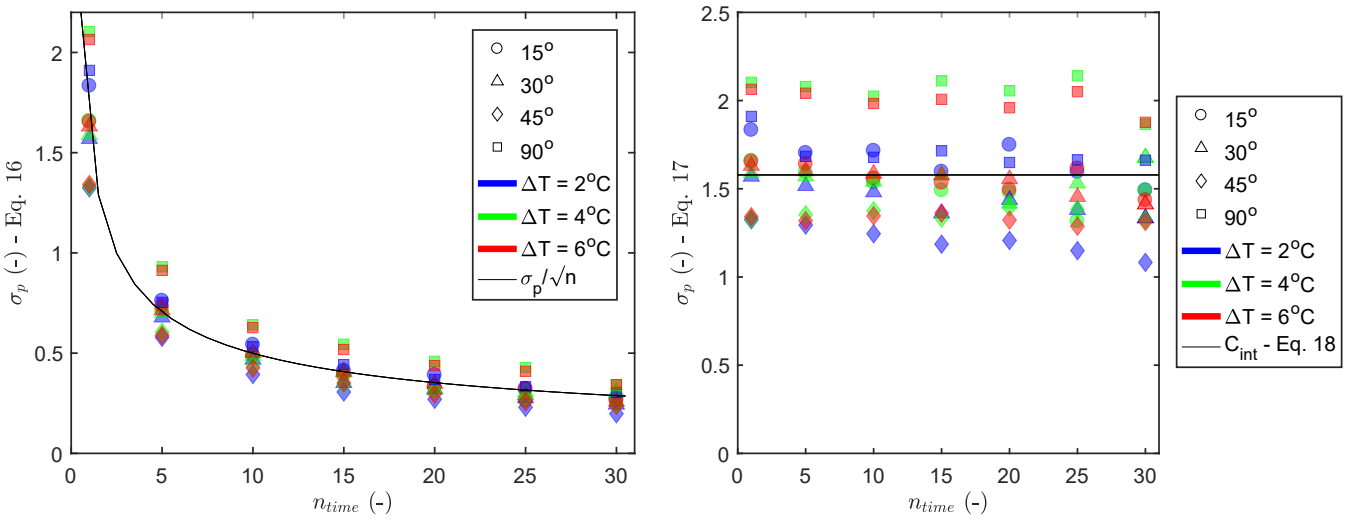

Figure 7. a) Precision of the AHFO wind speed measurements as a function of averaging period, independent of ΔT; and b) Precision of the AHFO wind speed measurements as a function of averaging period. Independent of ΔT and averaging period.

a DTS machine has different sampling resolutions. Furthermore it is possible to increase the precision of the observation by either averaging over space or time, depending on the scientific research question to be answered with AHFO. By using the shown $\frac{1}{\sqrt{n}}$ dependency, we can ~~easily~~ convert C_{int} into C_{DTS}, by multiplying C_{int} by $\sqrt{\frac{10}{1}}$, as ~~n is 10 times less.~~ n_{space} is 10. This results in Eq. 19 with n_{space}=1 and n_{time}=1. C_{DTS} is in our paper on purpose not calculated at once, but derived using C_{int}. As the wind speed in the middle of the wind tunnel can be assumed constant, we expect C_{DTS} to be better by using 5 measurements in the middle of the wind tunnel instead of picking one of these 5.

$$C_{DTS} = \overline{f(\bar{u}_j, n_{space}, n_{time}) \cdot \frac{\Delta T}{T_{error}} \sqrt{n_{time}}} \cdot \sqrt{n_{space}} = C_{int}\sqrt{10} = 1.6\sqrt{10} = 5.065.0 \tag{19}$$

3.2 Precision prediction

At the start of a new AHFO experiment it is unknown how to make sure the signal-to-noise ratio is sufficient, such that σ_p is small. However, given the result that the increase in precision behaves independent of ΔT and the averaging time, it is possible to make a prediction for the precision of future work.

In outdoor experiments, the only setting which can be changed is the heating rate, P_s, which is assumed to be fixed at a single value. The idea behind the precision prediction is to guide the choice of a heating rate, such that a preferred precision is achieved for a known dominant wind speed range. As the wind speed outside will vary naturally, ΔT will change accordingly. Therefore, to obtain an expression where P_s is the only unknown, ΔT first needs to be expressed as a function of the wind speed u_n and the heating rate (P_s). This can be done by using Eq. 10. To obtain a first estimate, some assumptions can be

made. The numerator of Eq. 10 consists of three terms, of which the first one with heating rate (P_s) is dominant compared to the other ones, namely 10-100 times bigger. When these minor terms are neglected Eq. 10 can be simplified to:

$$u_N = \left(\frac{0.5 P_s \pi^{-1} r^{-1}}{C d^{m-1} \mathrm{Pr}^n K_a \upsilon_a^{-m} (T_s - T_f)} \right)^{1/m} = \left(\frac{A P_s}{B \Delta T} \right)^{1/m} \tag{20}$$

With $A = 0.5\pi^{-1}r^{-1}$, $B = C(d)^{m-1}\mathrm{Pr}^n K_a \upsilon_a^{-m}$ and $\Delta T = T_s - T_f$, resulting in an expression for ΔT as a function of wind speed:

$$\Delta T = \frac{A P_s}{B u_n^m} \tag{21}$$

Knowing this expression of ΔT, Eq. 21 can again be rewritten into Eq. 22, which expresses the precision estimate, with P_s as only parameter which can be changed during an experiment.

$$\sigma_p(u_j, n_{space}, n_{time}, P_s) = C_{DTS} \frac{B T_{error} u_n^m}{A P_s} \sqrt{\frac{1}{n}} \sqrt{\frac{1}{n_{space} \cdot n_{time}}} \tag{22}$$

Where ~~n~~ $n_{space} \times n_{time}$ is the number of measurements over which the observed wind speed is averaged, in either space or time domain. By assuming that all constants are known from literature and the set-up, a first estimate of the error can be made for every velocity or heating rate given. If a dominant wind speed range for a new project is known, an associated heating rate can be found, such that the error is sufficiently small.

As an example, Figure 8 shows the estimated precision for our experiment at 1 s ~~and~~ ($n_{time} = 1$) and $\sim$ 0.675 m ($n_{space} = 10$) resolution over a range of wind speeds and heating rates. If the diameter of the fiber is different, this is taken into account via term A from Eq. 22, which includes the radius ($d = 2r$). Also, when a DTS machine with a different performance is used, this can be implemented by changing T_{error} accordingly. Of course different applications will demand different space-time averaging windows, depending on the scientific research question to be answered with AHFO, which option is included by $\sqrt{\frac{1}{n}}\sqrt{\frac{1}{n_{space} n_{time}}}$.

In outdoor experiments, the influence of the short and long wave radiation will be present. However, as long as the radiation is the same for the heated and non-heated segment, this does not influence the error estimation, as for the signal-to-noise ratio, ΔT is the most important factor. When the heated and reference fiber are close to each other, which is also needed for properly estimating the wind speed, both fibers will experience a similar contribution of external radiation, such that the overall ΔT will be relatively unaffected by this factor.

3.3 ~~Using~~ Considerations using AHFO outdoors

The experiments described here were performed in a controlled wind tunnel environment. When performing outdoor AHFO experiments, several factors need to be considered. First of all, during field experiments the relative humidity and temperature

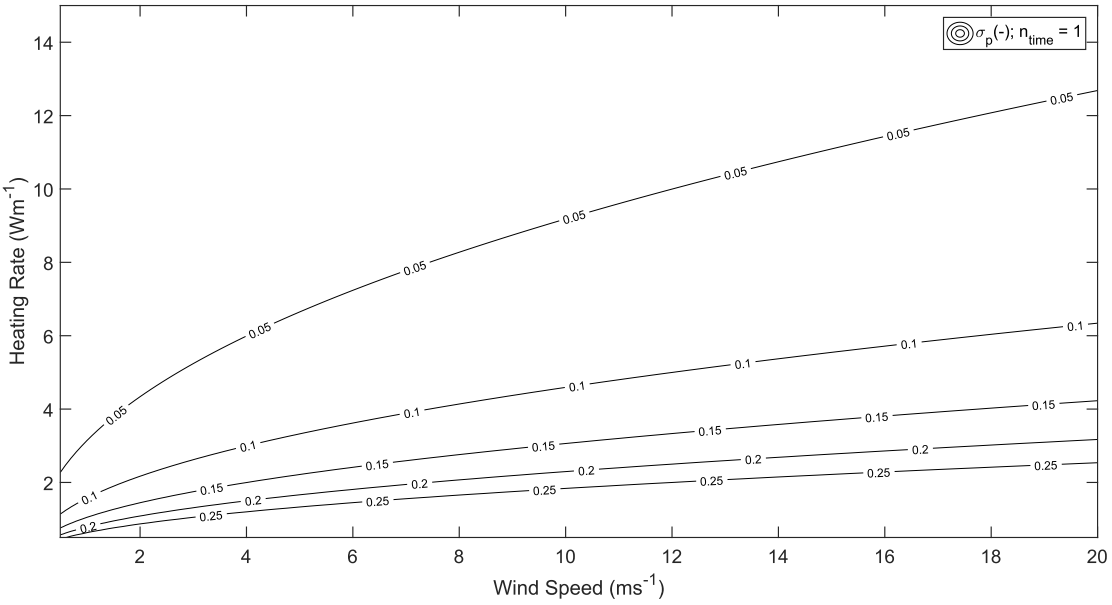

Figure 8. Expected precision (contour lines) for a given heating rate and wind speed as calculated from Eq. 22, with ~~a 1 s temporal resolution, averaged over 10 measurements~~$n_{space} = 10$ and $n_{time} = 1$.

might have such a big range that assuming certain parameters (e.g., K_a and υ_a) as constant is not applicable anymore (Tsilingiris (2008)). Furthermore, for small wind speeds (e.g., < 1 ms^{-1}), the neglection of energy losses like free convection seems not entirely applicable, as ~~is visible in the strong convergence of the contour lines in Figure 8~~this term becomes more dominant in comparison to forced convection. This is confirmed in our study, where it was visible that the response is different between a well ventilated and non-ventilated cable, hence the accuracy is dependent on the wind speed. Although not shown in this paper, it seemed there was no time response difference between a vertical or horizontal mounted heated cable, however by mounting the cable in a horizontal or vertical direction, free convection might influence the temperature measurements as the heated air is moving upward.

Also, the flow in the wind tunnel is laminar and has less turbulence than in outdoor conditions (Appendix B). This is a good setting for calibration of the AHFO method, however in outdoor conditions (small scale) turbulence around the cable is something to take into account. Especially with smaller wind speeds the cooling by turbulence around the cable can be an additional heat loss component, which is not included in the energy balance and therefore could lead to overestimation of the wind speed.

It is shown that AHFO can give reliable wind speed measurements, however the precision and accuracy is not as good as with a sonic anemometer. The major addition of AHFO is the possibility to sample the wind speed with a high spatial distribution. It should be taken into account that the time resolution is lower than that of a sonic anemometer and therefore AHFO is

less suitable for small scale turbulence, but turbulence can potentially be fully captured due to the setup with distributed measurements. Despite the high potential resolutions (1s and 0.3mm) the user should consider to average in either the space or time domain to enhance the precision of the obtained data. The choice for averaging over space or time should be made based on the researched topic.

Finally, when measuring in the field, the use of high quality reference point measurements (e.g., sonic anemometer) is recommended, for example to be able to compensate for possible biases. A sonic anemometer can also be useful to determine the angle of attack, as this is not (yet) possible with one single fiber. A more complex 3D set-up is necessary to be able to do this with DTS/AHFO (Zeeman et al. (2015)).

Despite these remarks, it will , something which would be interesting to perform outdoor tests in complex terrain, for both micrometeorological and hydrological applications, as AHFO gives a lot of insights in spatial varying wind fields. AHFO can be especially interesting in non-homogenous field sites, like forests, which are already studied with other DTS applications (Schilperoort et al. (2018)). Moreover, the ability to measure spatial varying wind fields can be useful for estimating sensible heat fluxes in a variety of atmosphere-vegetation-soil continuumsbe tested with AHFO in a field experiment.

4 Conclusions

Through a series of controlled wind tunnel experiments, new insights into the accuracy and precision of the newly introduced AHFO wind speed measuring technique were obtained. With high spatial (0.3 m) and temporal (1 s) resolution, the AHFO wind speed measurements agreed very well with the sonic anemometer measurements, with a coefficients of determination ranging from 0.85-0.980.94-0.99. It is also shown that the AHFO technique has the possibility to measure with a precision and accuracy of 95%. Some additional work is needed, as there still is a small overestimation, which may be caused by neglecting some energy fluxes, such as free convection due to heating of the air close the heated cable. Furthermore, it is possible to optimize the directional sensitivity compensation by extended calibration.

The error prediction equation (Eq. 22) is an important result of this work that will aid in the design of future experiments. This design tool helps with choosing a heating rate for the actively heated fiber in order to be able to create a sufficiently high precision. Based on the prevalent wind speeds of a potential field experiment site, a first estimate of an associated sufficient heating rate can be calculated. Due to the way this design tool is constructed, it can be generalized for all kinds of fibers, DTS precisions, and user preferred spatial and temporal resolutions.

The AHFO technique can reliably measure wind speeds under a range of conditions. The combination of high spatial and temporal resolution with high precision of the technique opens possibilities for outdoor application, as the key feature of the AHFO is the ability to measure spatial structures in the flow, over scales ranging from one meter to several kilometers. In the future, the technique could be useful for micrometeorological and hydrological applications in complex terrain, allowing for characterization of spatial varying fields of mean wind speed, such as in canopy flows or in sloping terrain.

Author contributions. Justus van Ramshorst prepared and performed the experiments, worked on analyzing the data and writing the manuscript. John Selker and Chad Higgins assisted with the experiments and analyzing the data and contributed to the manuscript. Miriam Coenders-Gerrits, Bart Schilperoort, Bas van de Wiel and Jonathan Izett helped with analyzing the data and contributed to the manuscript. Huub Savenije and Nick van de Giesen contributed to the manuscript.

Competing interests. The authors declare that they have no conflict of interest.

Acknowledgements. Many thanks for the practical assistance of Cara Walter and Jim Wagner with the AHFO/DTS setup and appreciation for the people of the OPEnS LAB for assisting with the assembling of parts. This project was partly funded by NWO Earth and Life Sciences, Veni project 863.15.022, The Netherlands. We are also grateful for the funding by Holland Scholarship and CTEMPs.

Appendix A: Comparison of AHFO and sonic anemometer wind speed

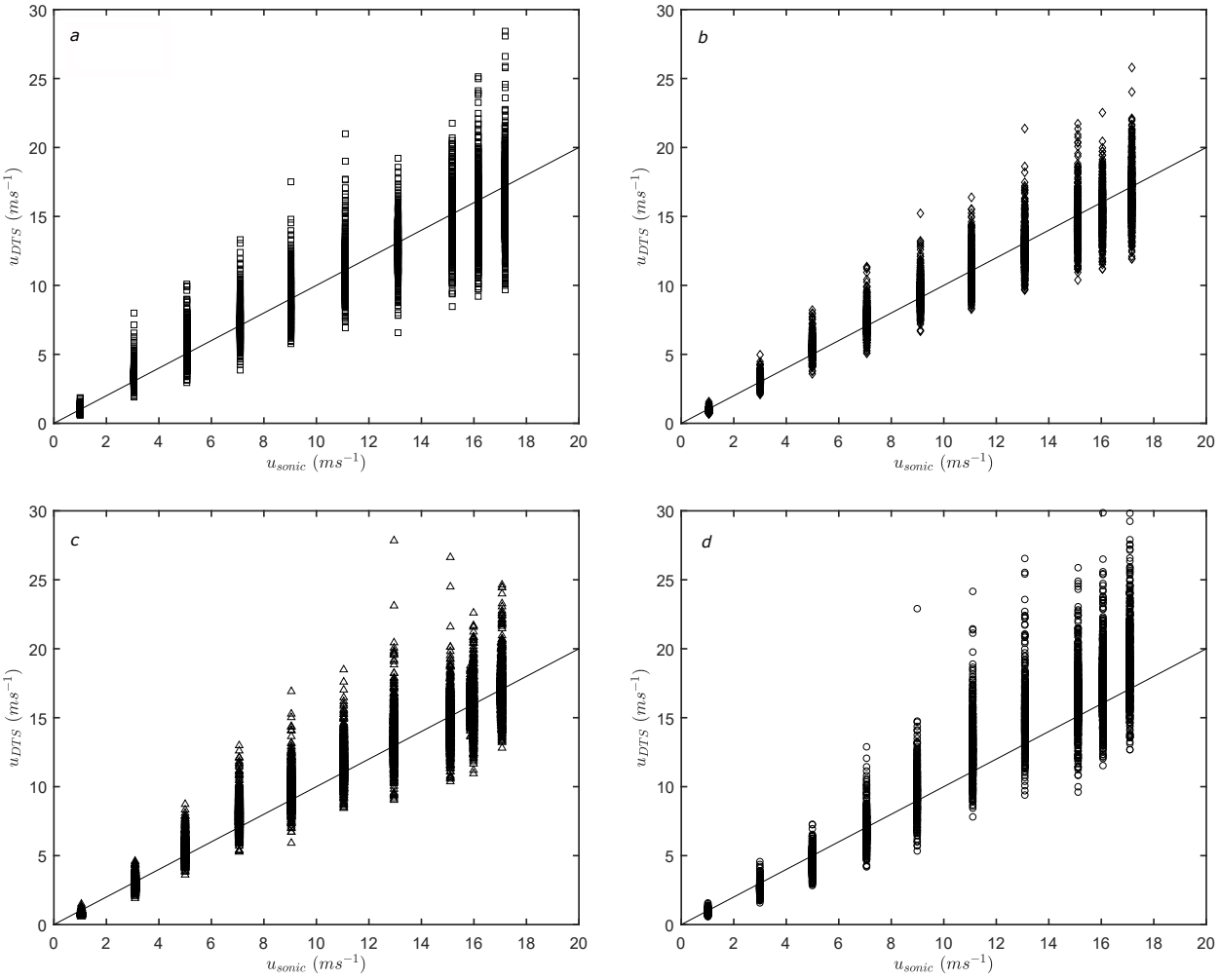

Figure A1. Comparison of AHFO and sonic anemometer wind speed at a 1 s temporal resolution, for the four different angles of attack. a) 90°, b) 45°, c) 30°, and d) 15°. $n_{space} = 10, n_{time} = 1$.

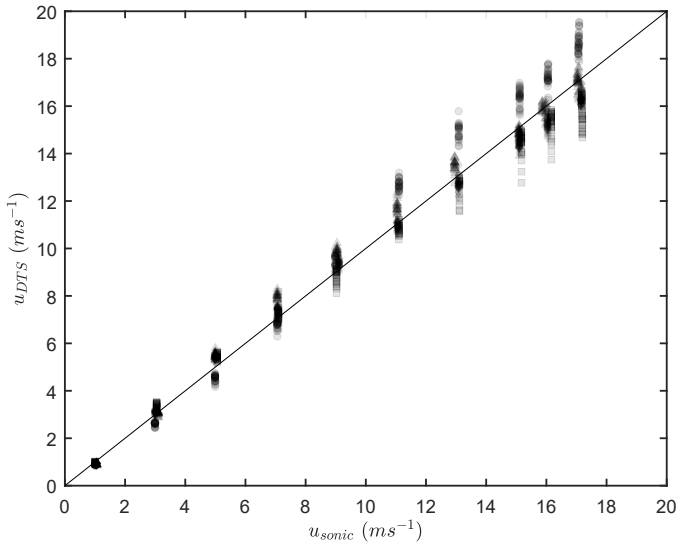

Figure A2. Comparison of AHFO and sonic anemometer wind speed averaged over 30 s for all angles of attack. $n_{space} = 10, n_{time} = 30$.

Appendix B: Wind tunnel flow characteristics

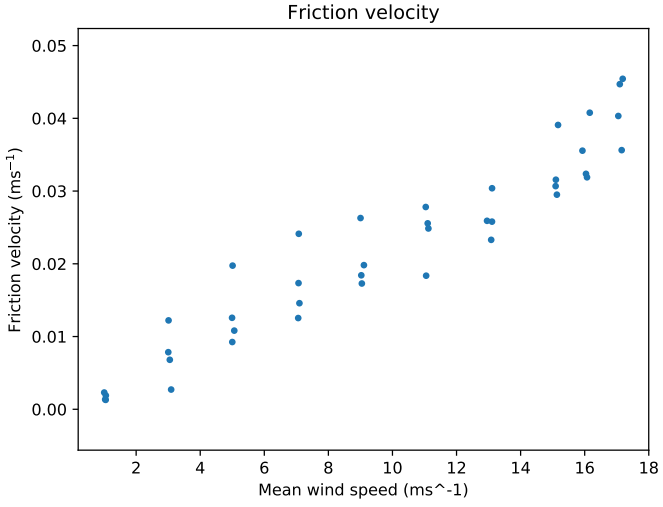

Figure B1. Friction velocity (ms^{-1}) in the wind tunnel during AHFO experiment.

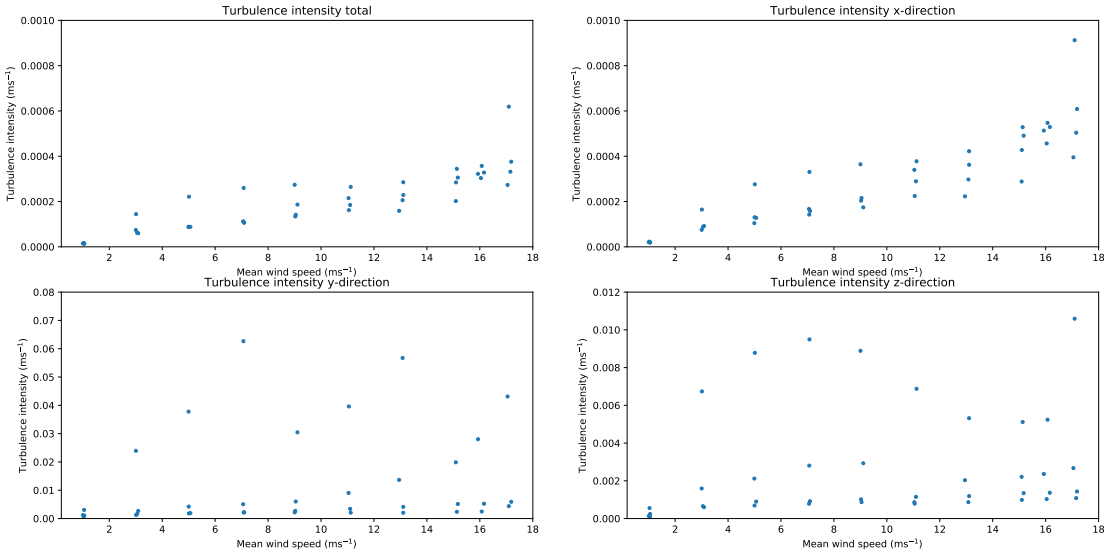

Figure B2. Turbulence intensity (ms^{-1}) in the wind tunnel during AHFO experiment.

Table C1. Standard deviation σ_{space} of 5 pairs of AHFO measurements (duplex configuration) per wind speed, and its normalized standard deviation. It shows that the normalized standard deviation is $\approx 3\%$ no matter if one takes the top, mid-top, center, mid-bottom, or bottom pair.

u (ms^{-1})	1	3	5	7	9	11	13	15	16	17
σ_{space} (ms^{-1})	0.033	0.092	0.147	0.181	0.235	0.312	0.323	0.445	0.526	0.544
Normalized σ_{space} (%)	0.033	0.031	0.029	0.026	0.026	0.028	0.025	0.030	0.033	0.032

For each angle and power rate, the u_{dts} was calculated with only the two temperature differences (duplex configuration) of the top of wind tunnel, or the mid-top, center, mid-bottom, or bottom of the wind tunnel (thus $n_{space} = 2$). From these 5 pairs we calculated the standard deviation σ_{space} per wind speed.

Appendix C: Extended spatial range

References

Adrian, R. J., Johnson, R. E., Jones, B. G., Merati, P., and Tung, A. T.: Aerodynamic disturbances of hot-wire probes and directional sensitivity, Journal of Physics E: Scientific Instruments, 17, 62–71, https://doi.org/10.1088/0022-3735/17/1/012, 1984.

Baldwin, A. J. and Lovell-Smith, J. E. R.: The emissivity of stainless steel in dairy plant thermal design, Journal of Food Engineering, 17, 281–289, https://doi.org/10.1016/0260-8774(92)90045-8, 1992.

Bou-Zeid, E., HIGGINS, C., HUWALD, H., MENEVEAU, C., and PARLANGE, M. B.: Field study of the dynamics and modelling of subgrid-scale turbulence in a stable atmospheric surface layer over a glacier, Journal of Fluid Mechanics, 665, 480–515, https://doi.org/10.1017/S0022112010004015, http://www.journals.cambridge.org/abstract{_}S0022112010004015, 2010.

Bruun, H. H.: Interpretation of a Hot Wire Signal Using a Universal Calibration Law., Journal of Physics E: Scientific Instruments, 4, 225–231, https://doi.org/10.1088/0022-3735/4/3/016, 1971.

Cengel, Y. and Ghajar, A.: Heat and mass transfer: fundamentals and applications, McGraw-Hill Higher Education, 2014.

Euser, T., Luxemburg, W. M. J., Everson, C. S., Mengistu, M. G., Clulow, A. D., and Bastiaanssen, W. G. M.: A new method to measure Bowen ratios using high-resolution vertical dry and wet bulb temperature profiles, Hydrology and Earth System Sciences, 18, 2021–2032, https://doi.org/10.5194/hess-18-2021-2014, 2014.

Goodberlet, M. A., Swift, C. T., and Wilkerson, J. C.: Remote sensing of ocean surface winds with the special sensor microwave/imager, Journal of Geophysical Research, 94, 14 547–14 555, https://doi.org/10.1029/JC094iC10p14547, 1989.

Ha, K.-J., Hyun, Y.-K., Oh, H.-M., Kim, K.-E., and Mahrt, L.: Evaluation of Boundary Layer Similarity Theory for Stable Conditions in CASES-99, Monthly Weather Review, 135, 3474–3483, https://doi.org/10.1175/MWR3488.1, http://journals.ametsoc.org/doi/abs/10.1175/MWR3488.1, 2007.

Hausner, M. B., Suárez, F., Glander, K. E., van de Giesen, N., Selker, J. S., and Tyler, S. W.: Calibrating single-ended fiber-optic raman spectra distributed temperature sensing data, Sensors, 11, 10 859–10 879, https://doi.org/10.3390/s111110859, 2011.

Higgins, C. W., Meneveau, C., and Parlange, M. B.: Geometric Alignments of the Subgrid-Scale Force in the Atmospheric Boundary Layer, Boundary-Layer Meteorology, 132, 1–9, https://doi.org/10.1007/s10546-009-9385-3, https://doi.org/10.1007/s10546-009-9385-3, 2009.

Higgins, C. W., Froidevaux, M., Simeonov, V., Vercauteren, N., Barry, C., and Parlange, M. B.: The Effect of Scale on the Applicability of Taylor's Frozen Turbulence Hypothesis in the Atmospheric Boundary Layer, Boundary-Layer Meteorology, 143, 379–391, https://doi.org/10.1007/s10546-012-9701-1, 2012.

Higgins, C. W., Wing, M. G., Kelley, J., Sayde, C., Burnett, J., and Holmes, H. A.: A high resolution measurement of the morning ABL transition using distributed temperature sensing and an unmanned aircraft system, Environmental Fluid Mechanics, 18, 683–693, https://doi.org/10.1007/s10652-017-9569-1, https://doi.org/10.1007/s10652-017-9569-1, 2018.

Hinze, J.: Turbulence, McGraw-Hill Higher Education, New York, 1975.

Holtslag, A. A., Svensson, G., Baas, P., Basu, S., Beare, B., Beljaars, A. C., Bosveld, F. C., Cuxart, J., Lindvall, J., Steeneveld, G. J., Tjernström, M., and Van De Wiel, B. J.: Stable atmospheric boundary layers and diurnal cycles: Challenges for weather and climate models, Bulletin of the American Meteorological Society, 94, 1691–1706, https://doi.org/10.1175/BAMS-D-11-00187.1, 2013.

Izett, J. G., Schilperoort, B., Coenders-Gerrits, M., Baas, P., Bosveld, F. C., and van de Wiel, B. J. H.: Missed Fog?, Boundary-Layer Meteorology, https://doi.org/10.1007/s10546-019-00462-3, http://link.springer.com/10.1007/s10546-019-00462-3, 2019.

Jong, S. A. P. D., Slingerland, J. D., and Giesen, N. C. V. D.: Fiber optic distributed temperature sensing for the determination of air temperature, pp. 335–339, https://doi.org/10.5194/amt-8-335-2015, 2015.

Kaiser, R. and Knight, W.: Digital signal averaging, Journal of Magnetic Resonance (1969), 36, 215–220, https://doi.org/10.1016/0022-2364(79)90096-9, http://linkinghub.elsevier.com/retrieve/pii/0022236479900969, 1979.

Keller, C. A., Huwald, H., Vollmer, M. K., Wenger, A., Hill, M., Parlange, M. B., and Reimann, S.: Fiber optic distributed temperature sensing for the determination of the nocturnal atmospheric boundary layer height, Atmospheric Measurement Techniques, 4, 143–149, https://doi.org/10.5194/amt-4-143-2011, http://www.atmos-meas-tech.net/4/143/2011/, 2011.

Kelly, M., Wyngaard, J. C., and Sullivan, P. P.: Application of a Subfilter-Scale Flux Model over the Ocean Using OHATS Field Data, Journal of the Atmospheric Sciences, 66, 3217–3225, https://doi.org/10.1175/2009JAS2903.1, http://journals.ametsoc.org/doi/abs/10.1175/2009JAS2903.1, 2009.

Madhusudana, C.: Accuracy in thermal contact conductance experiments - the effect of heat losses to the surroundings, International Communications in Heat and Mass Transfer, 27, 877–891, https://doi.org/10.1016/S0735-1933(00)00168-8, http://linkinghub.elsevier.com/retrieve/pii/S0735193300001688, 2000.

Patton, E. G., Horst, T. W., Sullivan, P. P., Lenschow, D. H., Oncley, S. P., Brown, W. O. J., Burns, S. P., Guenther, A. B., Held, A., Karl, T., Mayor, S. D., Rizzo, L. V., Spuler, S. M., Sun, J., Turnipseed, A. A., Allwine, E. J., Edburg, S. L., Lamb, B. K., Avissar, R., Calhoun, R. J., Kleissl, J., Massman, W. J., Paw U, K. T., and Weil, J. C.: The Canopy Horizontal Array Turbulence Study, Bulletin of the American Meteorological Society, 92, 593–611, https://doi.org/10.1175/2010BAMS2614.1, http://journals.ametsoc.org/doi/abs/10.1175/2010BAMS2614.1, 2011.

Perry, A.: Hot-wire anemometry, Clarendon press, Oxford, UK, 1982.

Petrides, A. C., Huff, J., Arik, A., van de Giesen, N., Kennedy, A. M., Thomas, C. K., and Selker, J. S.: Shade estimation over streams using distributed temperature sensing, Water Resources Research, 47, https://doi.org/10.1029/2010WR009482, http://doi.wiley.com/10.1029/2010WR009482, 2011.

Sayde, C., Buelga, J. B., Rodriguez-Sinobas, L., El Khoury, L., English, M., van de Giesen, N., and Selker, J. S.: Mapping variability of soil water content and flux across 1-1000 m scales using the Actively Heated Fiber Optic method, Water Resources Research, 50, 7302–7317, https://doi.org/10.1002/2013WR014983, http://doi.wiley.com/10.1002/2013WR014983, 2014.

Sayde, C., Thomas, C. K., Wagner, J., and Selker, J.: High-resolution wind speed measurements using actively heated fiber optics, Geophysical Research Letters, 42, 10 064–10 073, https://doi.org/10.1002/2015GL066729, 2015.

Schilperoort, B., Coenders-Gerrits, M., Luxemburg, W., Jiménez Rodríguez, C., Cisneros Vaca, C., and Savenije, H.: Technical note: Using distributed temperature sensing for Bowen ratio evaporation measurements, Hydrology and Earth System Sciences, 22, 819–830, https://doi.org/10.5194/hess-22-819-2018, https://www.hydrol-earth-syst-sci.net/22/819/2018/, 2018.

Selker, J., van de Giesen, N. C., Westhoff, M., Luxemburg, W., and Parlange, M. B.: Fiber optics opens window on stream dynamics, Geophysical Research Letters, 33, 27–30, https://doi.org/10.1029/2006GL027979, 2006a.

Selker, J. S., Thévenaz, L., Huwald, H., Mallet, A., Luxemburg, W., Van De Giesen, N., Stejskal, M., Zeman, J., Westhoff, M., and Parlange, M. B.: Distributed fiber-optic temperature sensing for hydrologic systems, Water Resources Research, 42, 1–8, https://doi.org/10.1029/2006WR005326, 2006b.

Steele-Dunne, S. C., Rutten, M. M., Krzeminska, D. M., Hausner, M., Tyler, S. W., Selker, J., Bogaard, T. A., and van de Giesen, N. C.: Feasibility of soil moisture estimation using passive distributed temperature sensing, Water Resources Research, 46, https://doi.org/10.1029/2009WR008272, http://doi.wiley.com/10.1029/2009WR008272, 2010.

Taylor, G. I.: The Spectrum of Turbulence, Proceedings of the Royal Society A: Mathematical, Physical and Engineering Sciences, 164, 476–490, https://doi.org/10.1098/rspa.1938.0032, http://rspa.royalsocietypublishing.org/cgi/doi/10.1098/rspa.1938.0032, 1938.

Thomas, C. K., Kennedy, A. M., Selker, J. S., Moretti, A., Schroth, M. H., Smoot, A. R., Tufillaro, N. B., and Zeeman, M. J.: High-Resolution Fibre-Optic Temperature Sensing: A New Tool to Study the Two-Dimensional Structure of Atmospheric Surface-Layer Flow, Boundary-Layer Meteorology, 142, 177–192, https://doi.org/10.1007/s10546-011-9672-7, 2012.

Tsilingiris, P.: Thermophysical and transport properties of humid air at temperature range between 0 and 100°C, Energy Conversion and Management, 49, 1098–1110, https://doi.org/10.1016/j.enconman.2007.09.015, http://linkinghub.elsevier.com/retrieve/pii/S0196890407003329, 2008.

Tyler, S. W., Burak, S. A., McNamara, J. P., Lamontagne, A., Selker, J. S., and Dozier, J.: Spatially distributed temperatures at the base of two mountain snowpacks measured with fiber-optic sensors, Journal of Glaciology, 54, 673–679, https://doi.org/10.3189/002214308786570827, https://www.cambridge.org/core/product/identifier/S0022143000208770/type/journal{_}article, 2008.

Tyler, S. W., Selker, J. S., Hausner, M. B., Hatch, C. E., Torgersen, T., Thodal, C. E., and Schladow, S. G.: Environmental temperature sensing using Raman spectra DTS fiber-optic methods, Water Resources Research, 45, 1–11, https://doi.org/10.1029/2008WR007052, http://doi.wiley.com/10.1029/2008WR007052, 2009.

van de Giesen, N., Steele-Dunne, S. C., Jansen, J., Hoes, O., Hausner, M. B., Tyler, S., and Selker, J.: Double-ended calibration of fiber-optic raman spectra distributed temperature sensing data, Sensors (Switzerland), 12, 5471–5485, https://doi.org/10.3390/s120505471, 2012.

Webster, C. A. G.: A note on the sensitivity to yaw of a hot-wire anemometer, Journal of Fluid Mechanics, 13, 307, https://doi.org/10.1017/S0022112062000695, http://www.journals.cambridge.org/abstract{_}S0022112062000695, 1962.

Zeeman, M. J., Selker, J. S., and Thomas, C. K.: Near-Surface Motion in the Nocturnal, Stable Boundary Layer Observed with Fibre-Optic Distributed Temperature Sensing, Boundary-Layer Meteorology, 154, 189–205, https://doi.org/https://doi.org/10.1007/s10546-014-9972-9, 2015.

Žukauskas, A.: Heat Transfer from Tubes in Crossflow, pp. 93–160, https://doi.org/10.1016/S0065-2717(08)70038-8, http://linkinghub.elsevier.com/retrieve/pii/S0065271708700388, 1972.